




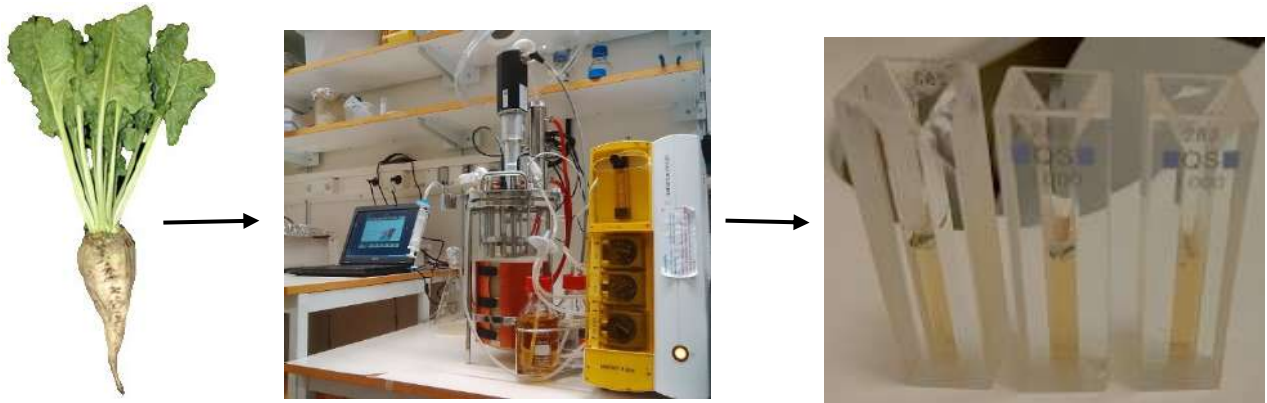
University of
Stavanger

Faculty of Science and Technology

MASTER'S THESIS

Study program/ Specialization: Biological Chemistry	Autumn semester, 2016 Spring semester, 2017 Open access
Writer: Damasus Chukwubueze Okeke	 (Writer's signature)
Faculty supervisor: Professor Peter Ruoff	
External supervisors: Dr. Nélida Leiva-Eriksson and Professor Leif Bülow	
Thesis title: Development of plant hemoglobin-based blood substitute: Fed-batch fermentation optimization and stability characterization	
Credits (ECTS): 60	
Key words: BvHb1.1-cTP, BvHb1.2, BvHb2, Hemoglobin, NsHb, Gateway technology cloning with clonase II mix, Fed-batch fermentation, Glucose feeding profile, Aeration rate, Purification, Ion exchange column, hydrophobic interaction column, Gel filtration column, SDS-PAGE, Autoxidation.	Pages: 50 + enclosure: 29 Stavanger, 13 July, 2017 Date/year

Development of Plant Hemoglobin-Based Blood Substitute: Fed-Batch Fermentation Optimization and Stability Characterization



Master of Science in Biological Chemistry

By
Damasus Chukwubueze Okeke

Spring 2017



Acknowledgement

This project work was carried out at Division of Pure and Applied Biochemistry, Lund University, Sweden, as part of her collaboration with University of Stavanger, Norway. I most sincerely appreciate this opportunity; it was a dream fulfilled.

It is by the Grace of God that everything was made possible. Therefore, I give utmost appreciation to His Holy Name.

First, I will like to thank my external supervisors, Professor Leif Bülow and Dr. Nélide Leiva-Eriksson for giving me opportunity to carry out my project work in their lab. Also, I will ever appreciate all your enormous support throughout the period of this master's thesis.

To all the staffs and other project students of the division; P-O, Johan, Karin, Ka, Ebba, Ulla, Alfia, Natali, and others that I could not mention their names here. I sincerely appreciate you all. You guys were very instrumental to the success of this work.

To my very good and supporting friend, Semhar Ghirmay, thank you for supporting me with your knowledge and experience during this work.

To the family I lived with at Veberöd, Sweden, I thank you so much for accepting me as your child, believing in me and giving me your great trust. It made my stay in your house comfortable and helped me to focus in my work.

To my family in Nigeria and most especially my senior brother, Denis Okeke, I appreciate you all for your care and support.

And finally, to my internal supervisor, Professor Peter Ruoff, thank you for all your support starting from the first day of my exchange studies at Lund University. I most appreciate your quick response and kind solutions to all my worries.

Abstract

The need for alternative blood substitutes is undoubtedly very enormous. Therefore, it is important to evaluate and develop different sources of starting material for this product. Focus has been on use of hemoglobin (Hb) from different sources, including human, whale etc. Following recent availability of genome sequence of sugar beet (*Beta vulgaris ssp. vulgaris*) effort is now put on studying three of its *hb* genes (*BvHb1.1*, *BvHb1.2*, and *BvHb2*) for their potentials in developing of hemoglobin-based oxygen carrier (HBOC). Unfortunately, these proteins are expressed in low amounts in plant. Consequently, use of recombinant biotechnology is an alternative way to obtain high amounts of these proteins. In this study, a fed-batch fermentation method was used in the production of recombinant *Beta vulgaris* Hbs (BvHbs). Five critical fermentation parameters were monitored while varying glucose feeding profile and aeration rate. Additionally, we characterized the autoxidation properties of one of these proteins, BvHb1.2, at different temperatures to examine its level of stability. Our result revealed that different conditions are favourable for cell growth and recombinant protein expression. A similar expression pattern of these proteins in plant was observed under fermentation. On the autoxidation assay, we could observe that high temperature facilitates autoxidation process. This implies that this protein can be preserved in its active form by maintaining it at low temperatures.

Finally, we conclude that different conditions are favourable for high yield fermentation of each of these proteins. In addition, appropriate culture glucose concentration and sufficient oxygen (O₂) level will reduce toxic by-product accumulation and provide high-cell density growth.

Table of Contents

ACKNOWLEDGEMENT	I
ABSTRACT	II
TABLE OF CONTENTS	III
ABBREVIATIONS	VI
LIST OF FIGURES	VII
LIST OF TABLES	VIII
1. INTRODUCTION	1
1.1. Aim of the study	1
1.2. Development of Recombinant Plant Hemoglobin-Based Blood Substitute	1
1.2.1. History of Substitute Development	1
1.2.2. Use of Recombinant Hemoglobin in Blood Substitute Development	3
1.3. Sugar Beet Hemoglobins	4
1.3.1. Plant Hemoglobins	4
1.3.2. Classification and Functions of Sugar Beet Non-Symbiotic Hemoglobins	5
1.3.3. Structural and Ligand-Binding Properties of Sugar Beet Non-Symbiotic Hemoglobins	7
1.4. Fed-Batch Fermentation of Recombinant (Plant) Hemoglobin	10
1.4.1. Glucose Metabolism in <i>Escherichia coli</i>	10
1.4.2. High-Density growth of <i>Escherichia coli</i> in Fed-Batch Fermenter	12
1.4.3. High-Level Expression and Production of Recombinant (Plant) Proteins in <i>Escherichia coli</i> by Fed-Batch Fermentation	13
1.5. Stability of Recombinant Sugar Beet Hemoglobin	14
1.5.1. Autoxidation	14
2. MATERIALS AND METHODS	16
2.1. <i>BvHb1.1</i> Cloning and Transformation of Expression Plasmid	16
2.1.1. Cloning of <i>BvHb1.1</i> Gene	16
2.1.1.1. Amplification and Preparation of pBSK- <i>BvHb1.1</i>	16

2.1.1.2. Subcloning of <i>BvHb1.1</i>	16
2.1.2. Transformation of Expression Plasmid	16
2.2. Fed-Batch fermentation and Expression of Recombinant Sugar Beet	
Hemoglobins	17
2.2.1. Fed-Batch Fermentation	17
2.2.2. Expression of Sugar Beet Hemoglobins	18
2.3. Analysis of Fermentation Sample	19
2.3.1. Glucose Concentration Measurement	19
2.3.2. Wet Cell Weight Determination	19
2.3.3. Lactic Acid Determination	19
2.4. Extraction and Purification of Recombinant Sugar Beet	
Hemoglobins	20
2.4.1. Extraction and Clarification	20
2.4.2. Purification	20
2.4.2.1. BvHb1.1-cTP Purification	21
2.4.2.2. BvHb1.2 Purification	22
2.4.2.3. BvHb2 Purification	23
2.4.3. Gel Electrophoresis of Sugar Beet Hemoglobins	23
2.5. Quantification of Hemoglobin and Heme Concentrations	24
2.5.1. Hemoglobin Quantification	24
2.5.2. Quantification of Heme Concentration	25
2.6. Stability Assay: Autoxidation	26
3. RESULT	28
3.1. Fed-batch Fermentation	28
3.1.1. Fermentation Data Analysis	28
3.1.1.1. BvHb1.1-cTP Fermentation Data Analysis	28
3.1.1.2. BvHb1.2 Fermentation Data Analysis	30
3.1.1.3. BvHb2 Fermentation Data Analysis	32
3.1.2. Batch Hemoglobin Yield Analysis	34
3.2. Sugar Beet Hemoglobins Purification	37
3.3. Autoxidation Assay	38
4. DISCUSSION	40
4.1. Fed-batch Fermentation of Sugar Beet Hemoglobins	40

4.2. Batch Fermentation Output: Cell Density and Hemoglobin	
Expression Yield	41
4.3. Purification of Sugar Beet Hemoglobins	42
4.4. Autoxidation of BvHb1.2	42
5. CONCLUSION	43
6. REFERENCES	44
7. APPENDICES	50

List of Abbreviations

Hb	Hemoglobin
FDA	Food and Drug Administration
O ₂	Oxygen
PFCs	Perfluorocarbons
RBCs	Red blood cells
rHb	Recombinant hemoglobins
LPS	Lipopolysaccharide
rHBOC	Recombinant hemoglobin-based oxygen carrier
BvHb	<i>Beta vulgaris</i> hemoglobin
LegHb	Leguminous hemoglobin
NsHb	Non-symbiotic hemoglobin
TrHb	Truncated hemoglobin
ATP	Adenosine triphosphate
DO	Dissolved oxygen
lpm	litre per min
wcw	wet cell weight
HGT	Horizontal gene transfer
MetHb	Methemoglobin
AcCoA	Acetyl Coenzyme A
PDHC	pyruvate dehydrogenase complex
PFL	Pyruvate formate lyase
ALDH	Acetaldehyde dehydrogenase
ADH	Alcohol dehydrogenase
LDH	Lactate dehydrogenase
QFF	Quaternary-sepharose Fast Flow
DEAE FF	Diethylaminoethanol-sepharose Fast Flow
BHP	Butyl high performance
QHP	Quaternary high performance
GE	Gel filtration
NaP	Sodium phosphate

List of Figures

- Figure 1. Structure of Hb molecule in the RBC
- Figure 2. Phylogenetic tree of plant Hbs
- Figure 3. Structural folds of nsHbs
- Figure 4. Tertiary structure of BvHbs
- Figure 5. Dimer interface in class 1 nsHb
- Figure 6. Types of Hbs
- Figure 7. Central glucose metabolic pathway in E. coli
- Figure 8. Structure of heme prosthetic group
- Figure 9. 5 L-capacity fermenter
- Figure 10. Äkta explorer protein purification system
- Figure 11. Spectrophotometric absorbance spectra of crude lysate CO-BvHb
- Figure 12. Heme spectrophotometric spectra
- Figure 13. Variation of five fermentation parameters in BvHb1.1-cTP fermentation
- Figure 14. Variation of five fermentation parameters in BvHb1.2 fermentation
- Figure 15. Plots of five fermentation parameters during fed-batch fermentation of BvHb2
- Figure 16. Harvested cell culture and cell pallets
- Figure 17. Hb yield mean \pm SD of BvHbs
- Figure 18. BvHbs after different purification steps
- Figure 19. SDS-PAGE result of each purification step
- Figure 20. Autoxidation determination of BvHb1.2

List of Tables

Table 1	Number of cycles and time for spectral autoxidation assay
Table 2	Estimated fermentation output of all batches
Table 3	Overall expression yield of BvHbs

1. INTRODUCTION

1.1. Aim of the Study

Cultivation of *E. coli* cultures has been the most common way to obtain high amounts of recombinant proteins which are considered to be low-volume-high-value products (Riesenberg et al., 1990). Sugar beet (*Beta vulgaris ssp. vulgaris*) hemoglobins are one of such products due to its envisaged potential to be used as starting material in hemoglobin-based oxygen carrier (HBOC) development. In a previous PhD dissertation work, recombinant *Beta vulgaris* hemoglobins were produced using traditional shake flask method and expression yield of about 20 – 25 mg per litre of culture was reported (Eriksson, 2014). Due to high amount of these proteins needed, the overall aim of this thesis is to use fed-batch fermentation method to obtain highest possible amount of these proteins. To achieve this, we intend to monitor effects of five critical fermentation parameters on both cell growth and target protein yield, and use results obtained to optimize yield. Additionally, we intend to characterize stability of these proteins base on their autoxidation rates at different temperatures.

1.2. Development of Recombinant Plant Hemoglobin-Based Blood Substitute

1.2.1. History of Blood Substitute Development

Blood is a crucial component of human life due to its primary role in the transportation of oxygen and carbon dioxide throughout the body. It is well understood that this function is carried out by red blood cells (RBCs). Hemoglobin (Hb), a metalloprotein present in the RBCs (Figure 1), is an oxygen-transporter responsible for oxygen distribution from the lungs to other tissues. The tremendous need for access to blood for life-saving purposes is of great concern globally. Situations such as surgery, child delivery, trauma, natural disasters, bleeding caused by serious injuries, and situations where blood cannot be giving due to religious or unavailability reasons, has stimulated interest over the development of alternative blood or “blood substitutes” (Alayash, 2014; Sarkar, 2008).

The world whole blood and packed red blood cells donation stand at an estimate of 103 million units with more than 15 million transfused in United States (Ness & Cushing) alone per annum (Varnado et al., 2013) leaving the rest of the world with only a small proportion. Even with that, there are increasing cases of blood shortage in U.S. medical services. The estimated blood donation rates in less-developing countries which stands for 0.4 units per thousand people compared to 85 units per thousand in the US is very worrisome (Varnado et al., 2013). Several factors such as handling regulations, increasingly stringent donor deferral criteria, and lack of blood donors are believed to have contributed to this problem (Kluger, 2010; Varnado et al., 2013). The situation has worsened with rising cases of blood-borne diseases, high cost of diagnosis, and adverse reactions arising from blood type incompatibility (Varnado et al., 2013).

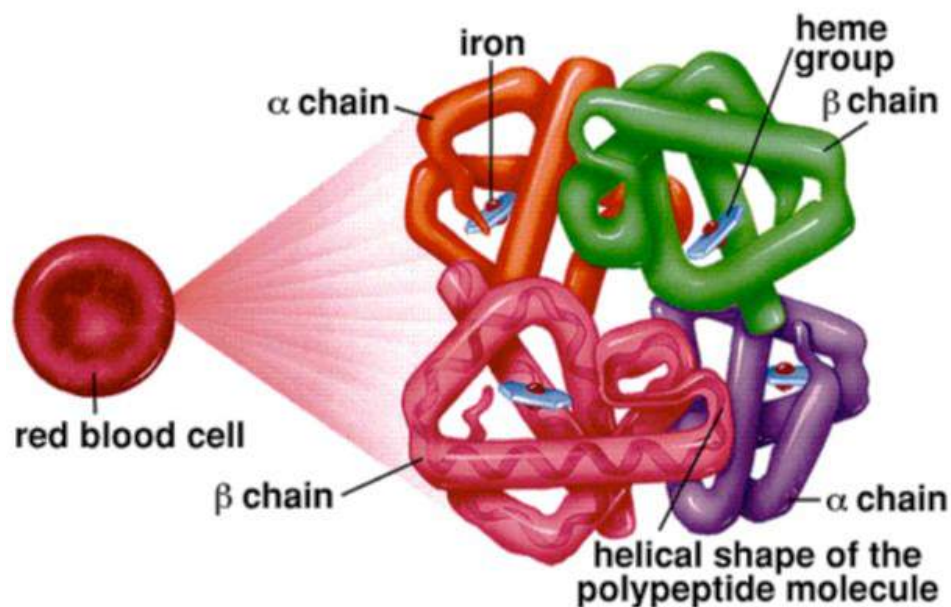


Figure 1. Structure of Hb molecule in RBC. The Hb is composed of four helical subunits; two α - and two β -chains. Each subunit contains an iron atom that reversibly binds an oxygen molecule. Picture obtained from fmss12ucheme.wordpress.com/2013/05/06/hemoglobin/ Collected on 17/05/2017.

The search for a viable and efficient blood substitute has been a continuous fight since more than 7 decades ago. This is due to persistent challenges surrounding early attempts. However, there are enormous foreseen health and economical potentials that any success in this field will provide. If successfully developed, blood substitute promises to be readily available, deliver a reasonable amount of oxygen, be free from transmitting infection, withstand long storage, compatible to all (Alayash, 2014; Sarkar, 2008), and serve as alternative to those who are sceptical about human blood transfusion. Many substances have been tried in the past as blood replacement including milk, saline solution, Ringer's solution (containing sodium, potassium, and calcium salts), Hb isolated from expired human blood and animal plasma (Sarkar, 2008). It has remained an ongoing struggle down the line as no product has been fully approved by the US Food and Drug Administration (FDA) (Grethlein, 2015). Fortunately, Hemopure, a polymerized form of bovine Hb, is currently being used in Russia and South Africa (Kluger, 2010). Other products have been developed to ameliorate health complications in which alternative blood is required, but they could not succeed due to their side effects (such as hypertension, abdominal pain, skin rash, diarrhea, jaundice, hemoglobinuria, oliguria, fever, and stroke) (Grethlein, 2015) and led to their withdrawal or failure at clinical trial stage (Sarkar, 2008).

A great effort is being dedicated by leading researchers in different parts of the world towards finding an alternative oxygen (O_2) transporter capable of replacing natural RBCs Hb function efficiently. Two different products have been under development as blood substitute. The first is based on perfluorocarbons (PFCs), a biologically inert material with high O_2 dissolution compare to blood plasma (Sarkar, 2008). PFCs consist of fluorine and carbon atoms, and is obtained by chemical polymerization reaction. Some advantages of PFCs are that it has high O_2 dissolution capacity, cheap to produce, and relatively safe as it can be produced devoid of any biological material. Also, if not completely metabolized in the body, PFCs are removed by exhalation (Grethlein, 2015). However, PFCs has some

disadvantages which includes; insolubility in water and inability to carry enough O₂ (Sarkar, 2008).

The second product under development by researchers and most advanced in clinical trials phase (Grethlein, 2015) are Hb-based products, which is expected to mimic the O₂ transport function of mammalian RBCs Hb (Sarkar, 2008). A study conducted in the 1940s revealed that native (stroma-free) Hb is not antigenic, is more stable upon sterilization, and has longer shelf-life compare to RBCs. But on the other hand, due to the absence of 2, 3-bisphosphoglycerate which allosterically triggers oxygen release at half O₂ saturation pressure (p-50), the oxygenation and release efficiency of Hb is a problem. There is also risk of dimerization of free Hb resulting to glomerular filtration clearance and reticuloendothelial system absorption (Grethlein, 2015). Apart from that, there are also some challenges surrounding this product such as; form of delivery due to toxicity concern, and its stability in solution. Report has shown that through either chemical cross-linking or use of recombinant DNA technology or both, a product with enhanced properties can be developed (Sarkar, 2008).

1.2.2. Use of Recombinant Hemoglobins in Blood Substitute Development

Recombinant hemoglobins (rHb) and other naturally occurring Hbs have been reported to be a potential starting material for alternative blood development (Fronticelli & Koehler, 2009). By definition, rHb consist of concentrated solutions of purified stroma-free Hb, which has been heterologously expressed in transgenic bacteria, mice, swine, yeast, or other organisms (Varnado et al., 2013). Products of this material are believed to possess improved properties over packed RBCs in certain critical functions such as; longer shelf-life, and enhanced O₂ delivery, among others (Varnado et al., 2013). However, issues related to expression and purification some of which includes; globin denaturation, misfolding, heme-disorientation, antigenic *E. coli* lipopolysaccharide (LPS) removal, protein impurities, and modified heme is of great concern (Plomer et al., 1998). Since rHb are obtained in stroma-free and unmodified form, it has been reported that transfusing acellular Hb into humans could lead to health complications including renal failure and oxidative stress resulting from renal clearance and instability-associated reactivity of dimers (Bunn, Esham, & Bull, 1969; Fronticelli & Koehler, 2009; Kresie, 2001; Sanders, Ackers, & Sligar, 1996). Also, cell-free Hb show different oxygen transport properties when compared with whole blood or packed RBCs Hb (Varnado et al., 2013). Consequently, chemical modification by polymerization, modification by encapsulation into vesicles and genetic fusion of subunits (Ness & Cushing, 2007) might be required to prevent endothelial extravasation and increase O₂-carrying capacity. Cross-linking by PEGylation (polyethylene glycol polymers) can also be used to improve stability and retention along the kidney glomerular filters (Fronticelli & Koehler, 2009).

1.3. Sugar Beet Hemoglobins

1.3.1. Plant Hemoglobins

Soybean was the first plant in which Hb was identified (Garrocho-Villegas, Gopalasubramaniam, & Arredondo-Peter, 2007). In his work, Kubo isolated a red pigment from root nodule of soybean, crystallized the hemin from the pigment, and was able to show that it is identical to that of horse Hb, concluding that this pigment is a hemoprotein. Kubo observed through his experiment that this protein facilitates O₂ transport and its assimilation by the N₂-fixing bacteria present in the nodules. The physiological role of leghemoglobin (LegHb) in legumes were further clarified to involve maintaining internal O₂ concentration low enough to avoid inhibitory effect on O₂-sensitive nitrogenase (Garrocho-Villegas et al., 2007). This Hb was later named LegHb as it was found in leguminous plant (Virtanen & Laine, 1946). Today, Lb is also known as symbiotic Hb (sHb). Following this, search for presence of Hb in non-leguminous plants went through many biochemical and molecular biology methods for several years without success. In 1982, Jeffrey hypothesized that plant Hbs originate through horizontal gene transfer (HGT) from a phytophagous insect to a primitive legume via a viral vector (Jeffrey, 1982). This assertion was later overthrown by several evidences on vertical evolution hypothesis that indicated the possibility of finding Hb in all land plants (Veronica et al, 2007). Identification of Hb in *parasponia*, a non-leguminous nodulating plant, gave a strong support for this hypothesis. Later, Hb was also identified in actinorhizal plants (plants with symbiotic association with actinobacteria, Frankia) such as *Casuarina cunninghamiana* and *Myrica gale* (Tjepkema, 1983), and non-symbiotic plants, such as *Trema* and *Celtis* (Veronica et al, 2007). These findings revealed that Hb exists across all land plants and supports their occurrence from a single ancestor through vertical evolution. In 1990s, the cDNA of barley and maize (monocots) non-symbiotic Hbs (nsHbs) were cloned and sequenced, and showed that their amino acids sequence was 71 % similar to Hbs of *parasponia* (Raúl Arredondo-Peter, Hargrove, Moran, Sarath, & Klucas, 1998). In 1997, Arredondo-Peter and his colleagues reported their work on two genes from rice and compared their sequences with other Hbs. They proposed that their proteins were 93 % identical, 68 – 82 % identical to other nsHbs, and about 50 % identical to sHbs. The recent availability of genome sequencing technology has led to identification of Hbs in many plant, even in primitive ones (R. Arredondo-Peter et al., 1997).

Three types of Hbs have been identified in plants; sHbs, nsHbs, and truncated (2/2) Hbs (tHbs) (Ross et al., 2002). These Hbs has been isolated from different plants species and characterized for their physiological roles and structure. NsHbs has been suggested to play a role in cell metabolism and plant stress response(Garrocho-Villegas et al., 2007). Regarding trHbs, Vinogradov et al., (2006) showed in their phylogenetic analysis that these truncated 2/2-like Hbs are more closely related to bacterial 2/2 Hbs than to sHbs or nsHbs. Although the structure of Hbs has been elucidated, its biological function remains unknown. Watts and his colleagues proposed their function to be O₂-transport though (Watts et al., 2001).

1.3.2. Classification and Functions of Sugar Beet Non-Symbiotic Hemoglobins

NsHbs have been divided into two classes, namely; class-1 (nsHb1) and class-2 (nsHb2) (Figure 2) based on phylogenetic analysis, expression pattern and ligand binding features (Hunt et al., 2001). Both classes of nsHbs are not evenly distributed across plant species. One or more nsHb1 has been commonly identified in monocots. In dicots, both classes of nsHbs exist and carry at least one class-1 nsHb and one class-2 nsHb, except in legumes and other non-symbiotic nodulating plants where class-2 nsHb has evolved into sHb (Garrocho-Villegas et al., 2007; Hunt et al., 2001; Smagghe et al., 2009). Furthermore, these classes of nsHb has been identified to exhibit different expression patterns depending on organ and developmental stage of plant (Leiva-Eriksson et al., 2014) and, to have different structural and ligand association characteristics (Eriksson, 2014; R. D. Hill, 2012; Hunt et al., 2001). There is growing evidence that they may have a role in seed development and germination, flowering, root development and differentiation, abiotic stress responses, pathogen invasion and symbiotic bacteria association (R. D. Hill, 2012).

With that, three *nshb* genes was recently identified in sugar beets following genomic sequencing analysis. Based on sequence differences, *Bvhb1-1* and *Bvhb1-2* belong to nsHb1 whereas *Bvhb2* belongs to nsHb2 (Figure 2). The fourth sugar beet *hb* gene, *Bvhb3*, is a member of trHbs group. Following the work on the crystal structure of trHb from *A. thaliana*, a non-symbiotic plant, this gene was reported to belong to class-3 nsHb (nsHb3) (Reeder & Hough, 2014).

The role of nsHbs in plants have not been clearly defined due to overlapping features in their sequence, structures and ligand binding kinetics (Eriksson, 2014). However, evidences are growing on the probability that BvHbs and other nsHbs might have physiological roles other than or in addition to O₂ transport. This is due to observed ligand kinetics, their localization in metabolically active tissues and amount found in stressed tissues (Garrocho-Villegas et al., 2007). There are several reports on expression of nsHbs in different part of plant, including; seeds, roots and other organs, and under certain abiotic conditions, such as cold and hypoxia (Robert D. Hill, 1998; R. D. Hill, 2012; Thiel et al., 2011). According to Arredondo-Peter et al., (1998), nsHbs carry out three major physiological roles in plant metabolism; exogenous ligands binding (which aids in regulating cell metabolism as a result of interactions with other molecules), small organic molecules binding, (such as fatty acids, thereby playing a role in their synthesis and transport), and act as O₂ scavenger through their strong interaction with O₂. NsHbs have also been implicated to be involved in regulating ATP levels in the cell under hypoxia conditions (Sowa, Duff, Guy, & Hill, 1998). Class-2 nsHbs, specifically, has been proposed to have a role in mediating O₂ diffusion to some plant tissues due to their low O₂ affinities (Smagghe et al., 2009). From their work on NO production in alfalfa root culture kept under low O₂ concentration using high Hb expressing cell lines and low Hb expressing cell lines, Dordas and his colleagues observed more than 2.5-fold increase in NO production in low Hb expressing culture (Dordas et al., 2003). This was also confirmed by report on NsHb1 from *A. thaliana* role in NO scavenging under hypoxic condition, where it regulates NO level in the cell (Perazzolli et al., 2004). There is presently no available information on the specific role of BvHbs, but as a member nsHbs family with certain shared features observed in other members of this family (such as *A. thaliana*, barley, rice

etc) that have been extensively studied. We believe that their physiological role will not be far from those enumerated above.

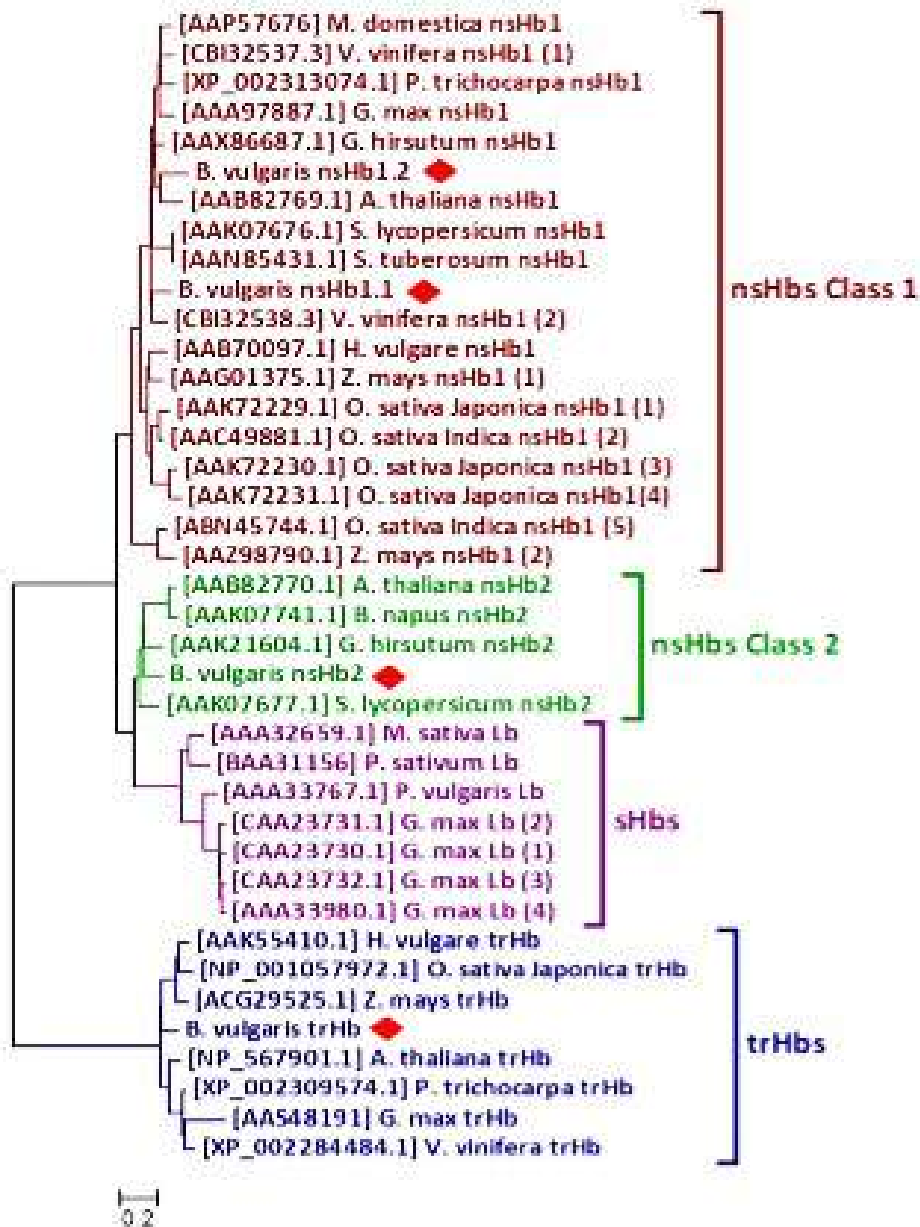


Figure 2. Phylogenetic tree of plant Hbs. The plant Hbs are classified into four groups. And the four BvHbs (*B. vulgaris* nsHb1.1, *B. vulgaris* nsHb1.2, *B. vulgaris* nsHb2, and *B. vulgaris* trHb) are indicated in red diamond. Figure adapted from (Eriksson, 2014).

1.3.3. Structural and Ligand-Binding Properties of Sugar Beet Non-Symbiotic Hemoglobins

NsHbs possess the characteristic myoglobin-fold structure common among many Hbs found in different organisms. This structure consists of eight alpha helices represented by letters A to H. Helices E and F, respectively, contain the distal and the proximal histidines which coordinates Fe of the heme group, and are conserved across globin family (Hoy & Hargrove, 2008; Spyraakis, Luque, & Viappiani, 2011). NsHbs exhibit two different structural fold; a 3-on-3 typical myoglobin-fold (Figure 3A) seen in class-1 nsHb as well as class-2 nsHb and a 2-on-2 fold (Figure 3B) seen in class-3 nsHb. The 2-on-2 fold of nsHb3 has been attributed to incomplete helices and some structural disarrangement peculiar to this kind of Hbs (Mot, 2014).

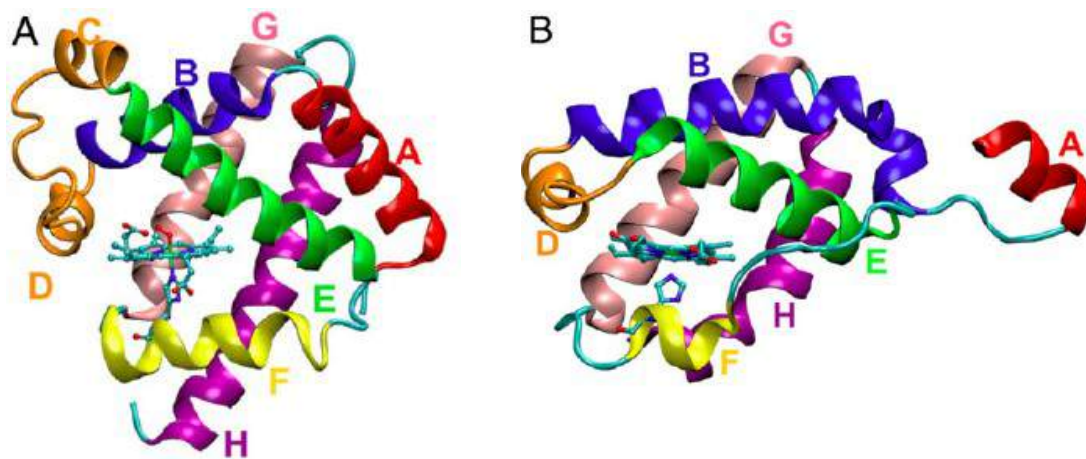


Figure 3. Structural folds of nsHbs. A) 3-on-3 typical myoglobin-fold common among class 1 and class 2 nsHbs. B) truncated 2-on-2 Hb fold similar to bacterial Hb structure. The eight alpha helices are labeled with letters A – H. The structure was adapted from (Capece et al., 2013).

RiceHb1 was the first nsHb whose crystal structure was resolved (Hargrove et al., 2000). Extensive work on this group of Hbs has been done on monocots' class-1 nsHbs from barley, rice and corn (Hoy & Hargrove, 2008). In dicotyledons, AtHb1 is the most studied class-1 nsHb of this group. Not so much is known about the structure of class-2 nsHb. Although cornHb2 and Athb2 were recently characterized (Bruno et al., 2007; Garrocho-Villegas et al., 2007), no crystal structure of class-2 nsHb has been resolved (Kakar et al., 2011). The structures of the three nsHbs present in sugar beet (BvHbs) were obtained by computational homology modelling. According to Eriksson et al., (2014), both sugar beet class-1 nsHbs (BvHb1.1 and BvHb1.2) structures were modelled using the X-ray structures of TremaHb and AtHb1. And sugar beet nsHb2 (BvHb2) structure was modeled using the X-ray structures of AtHb1 and LegHb of yellow lupin that shows highest sequence identity to the BvHb2 sequence. The result of the modelling reveals typical globin fold comprised (Figure 4). Furthermore, the well reported 3-on-3 canonical helical arrangement as well as the position of the heme group were similar to that earlier reported. There is also report on class-1 nsHb been a homodimer and class-2 nsHb a monomer. This is supported by the structural arrangement and nature of amino acid residues around the

surface of interaction between comprising subunits. Class-1 BvHbs exhibit a ring-shaped contact interface between the two subunits with amino acid residues capable of forming hydrogen bonds (GluG7-ThrC3) as well as electrostatic interaction (GluG4-HisG5) and (GluB15-LysH5). There is also extra ValG2 present in BvHb1.2 but absent in BvHb1.1 that provides extra stability for the homodimer (Figure 5) (Eriksson, 2014).

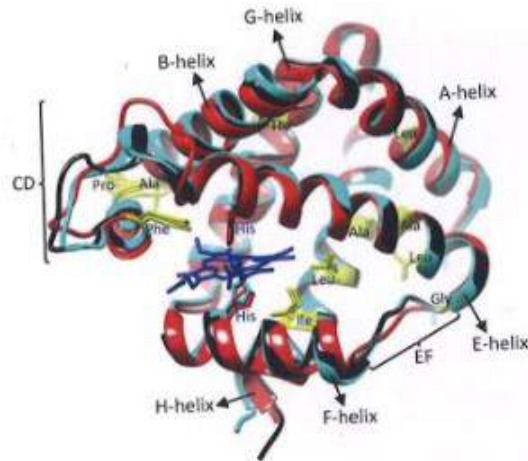


Figure 4. Tertiary structure of BvHbs. Front view of the modelled structures of BvHb1.1 (black), BvHb1.2 (cyan), and BvHb2 (red). Amino acid residues that are highly conserved across plant species are shown in yellow. The ones surrounding the heme group are in blue. Heme group is shown also in blue. Amino acid residues that (probably) participate in maintaining globin structure is presented in black. The structure was adapted from (Eriksson, 2014).

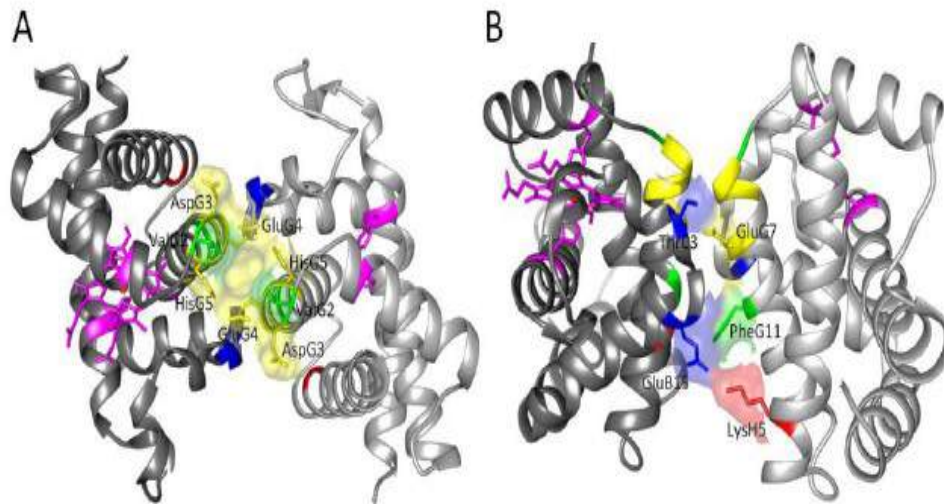


Figure 5. Dimer interface in class 1 nsHb. A). Upper view of the dimer showing amino acid residues in the G helix that is involve in dimerization. These residues include; AspG3, GluG4, and His G5. B) Front view of the dimer showing other residues that interact, they are; ThrC3 – GluG7, and LysH5 – GluB15. The structure was adapted (Eriksson, 2014).

The variations in the structures of BvHbs underline the observed differences in ligand binding behaviour and biological functions exhibited by these proteins. The heme pocket

area is of much interest when considering the reactivities of these proteins with exogenous ligands. Hbs can be pentacoordinate (Figure 6A) or hexacoordinate (Figure 6B) based on their iron coordination. O₂-transporting Hbs of plants and animals possess purely pentacoordinated heme iron. NsHbs are hexacoordinated (Kakar, Hoffman, Storz, Fabian, & Hargrove, 2010).

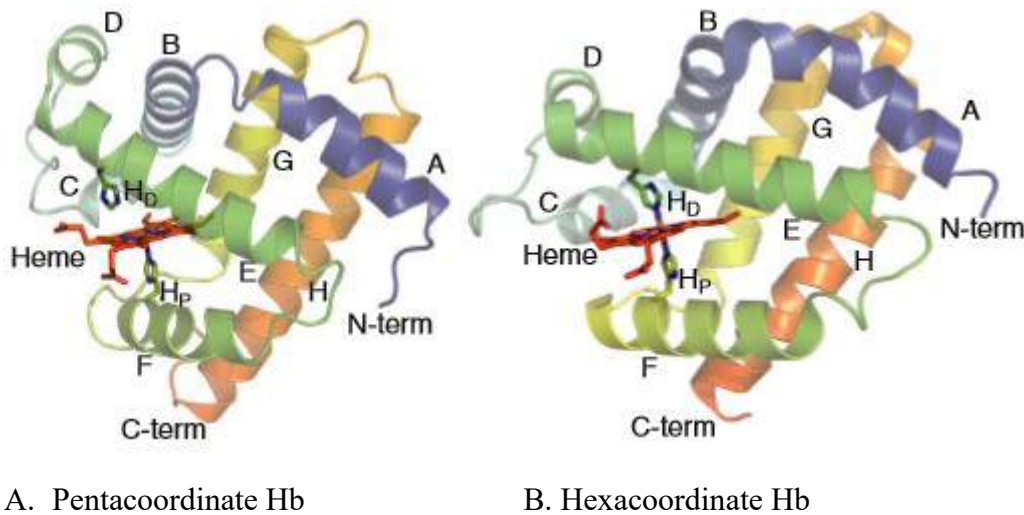


Figure 6. Types of Hbs. A. pentacoordinate Hb, and B. hexacoordinate Hb. Both Hbs differ from each other based on extra distal histidine coordination observed in hexacoordinate Hb. Adapted from (Kakar et al., 2010).

Although both class-1 and class-2 BvHbs are hexacoordinated, class-1 has much less affinity for the distal histidine than class-2, and thus is less hexacoordinated. There are many reports on high oxygen affinities and low oxygen dissociation rate constants among class-1 nsHbs (Kakar et al., 2010). Phenylalanine from the helix-B in riceHb1 was mutated, and it was revealed that this amino acid plays a role in destabilizing hexacoordination. This suggesting that Phe is responsible for less hexacoordination character observed in class 1 nsHbs (Smagghe et al., 2009). Kakar and his colleagues have described how distal histidine influences the rate of ligand binding. This statement has been confirmed by a report where ligand binding in hexacoordinated Hbs was found to be more complex than in pentacoordinated Hbs. The reason is due to the competition between the exogenous ligands and the intramolecular coordination of the distal histidine that blocks the ligand binding site (Hargrove et al., 2000; Smagghe, Sarath, Ross, Hilbert, & Hargrove, 2006). This is reflected in the class-2 nsHb which has been reported to be dominantly hexacoordinated with a low oxygen affinity (Mot, 2014) and high oxygen dissociation rate constants due to effects of distal histidine (R. Arredondo-Peter et al., 1997; Hargrove et al., 2000). In the case of BvHbs, Eriksson and her colleagues reported in their laser flash photolysis experiment on CO binding with BvHbs a lower CO binding rate for BvHb2 than those obtained for class-1 BvHbs. And stated further that this could be due to presence of AsnB1 and GluB4 residues at the same position as observed in other class-1 nsHbs. Affinity of O₂ to BvHbs and other plant nsHbs depends on two factors; degree of hexacoordination and rate of dissociation of bound O₂. BvHb2 with stronger

hexacoordination has lower oxygen affinity compared to class-1 BvHbs, but quite similar to that obtained with BvHb1.2 (Eriksson, 2014).

1.4. Fed-batch Fermentation of Recombinant (Plant) Haemoglobin

1.4.1. Glucose Metabolism in *Escherichia coli*

Glucose is the most common carbon source used for cultivation of *E. coli* and other bacteria because glucose supports rapid growth (Bren et al., 2016). Xylose and glycerol are also other carbon sources used. *E. coli* is a gram-negative facultative anaerobe capable of metabolizing energy under both aerobic and anaerobic conditions (Wikipedia, 2016). Glucose uptake into cells involves some transporting channels which include; phosphotransferase system (PTS), and galactose-proton-symport system (Chen, Yap, Postma, & Bailey, 1997). Under aerobic conditions, glucose is metabolized via glycolysis pathway and pentose phosphate pathway (PPP) to produce ATP, reducing power (NADH) and pyruvate (Murarka, Clomburg, Moran, Shanks, & Gonzalez, 2010). Pyruvate is the metabolic node and point of interchange between respiratory and fermentative metabolism in cells.

In the presence of O₂, pyruvate enters tricarboxylic acid (TCA) cycle in form of acetyl coenzyme A (AcCoA) and undergo oxidative reactions generating carbon dioxide and reducing power (NADH) necessary for ATP production via coupling to electron transport systems and oxidative phosphorylation. On the other hand, under anaerobic fermentation, pyruvate formate-lyase (PFL) replaces the activity of pyruvate dehydrogenase complex (PDHC) that converts pyruvate to AcCoA by converting pyruvate to both formate and AcCoA. The AcCoA formed is further reduced to ethanol by alcohol dehydrogenase (ADH) through a series of reactions. Also, the AcCoA formed in the fermentative metabolism of glucose is directed towards energy (ATP) generation by the activities of phosphate acetyltransferase (PTA) and acetate kinase, and finally generates acetate. Another important toxic by-product of fermentative glucose metabolism is lactate. Lactate is secreted through reductive activity of lactate dehydrogenase using NADH as proton (H⁺) donor (Figure 7). When O₂ is absent, pyruvate produced from glycolysis is converted to a mixture of organic acids (acetate, formate, lactate, and succinate), ethanol, carbon dioxide (CO₂), and hydrogen (H₂) (Figure 7) (Murarka et al., 2010).

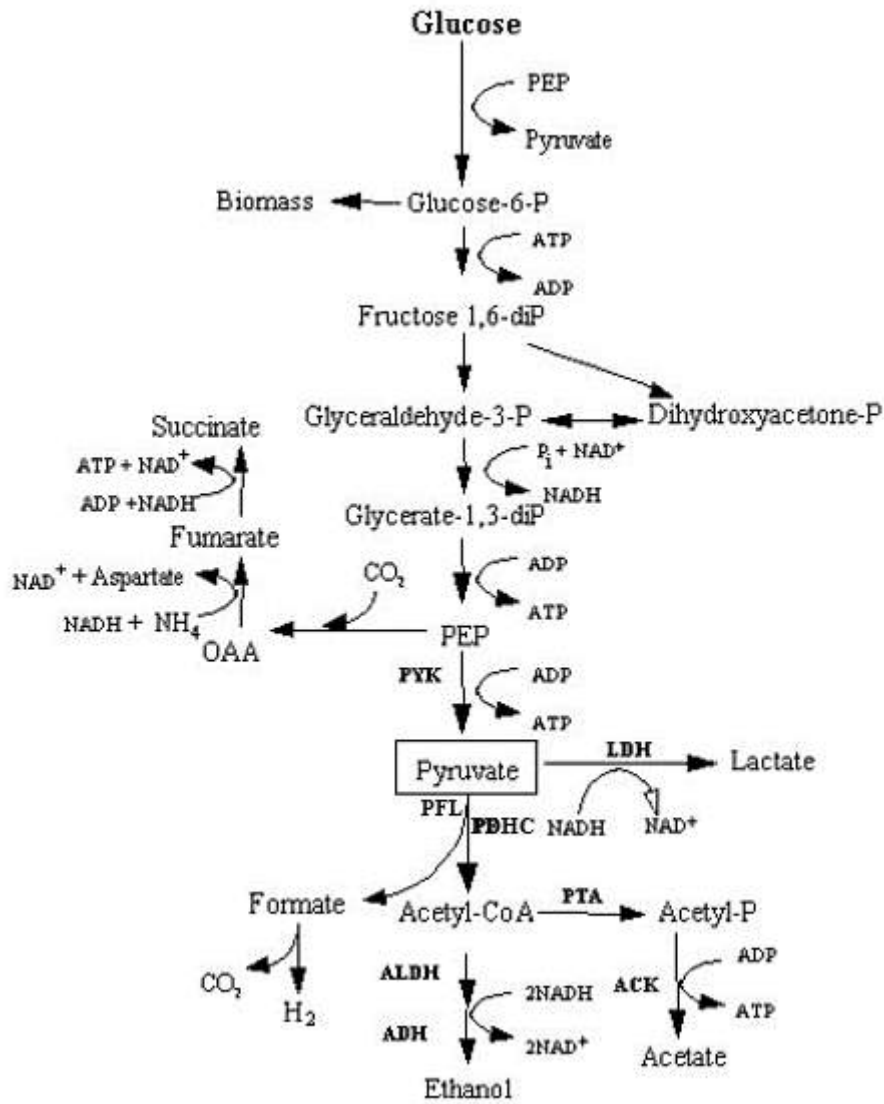


Figure 7. Central glucose metabolic pathway in *E. coli*. Enzymes involved in the pyruvate dissimilation as well as fermentation include; pyruvate formate-lyase (PFL), pyruvate dehydrogenase complex (PDHC), alcohol dehydrogenase (ADH), pyruvate acetyltransferase (PTA), acetate kinase (ACK), and lactate dehydrogenase (LDH). Adapted from (Yang, Bennett, & San, 1998) and slightly modified.

1.4.2. High-density growth of *Escherichia coli* in Fed-batch Fermenter

As early as 1970s researchers had recognized the need for growing high-density bacterial cultures to achieve maximum productivity. As a result, several approaches have been developed including; improving media composition and feeding techniques, manipulating the bacteria's physiology, and improving cultivation techniques (such as batch, fed-batch, and dialysis fermentation methods) (J. Shiloach & Fass, 2005). The first attempt to grow high-density bacteria culture dates as far back as 1943 when Hestrin and his colleagues reported their work on cultivation of bacteria using a cellophane sac in order to separate the culture from a pool of nutrients (Hestrin, Avineri-Shapiro, & Aschner, 1943). In 1963, the first ever dialysis fermentation system capable of exchanging low molecular weight molecules in the growth medium and taking in fresh nutrients, including O₂ was developed. With this, cell density of about 148 g/l dry cell weight (dcw) could be achieved (Gallup & Gerhardt, 1963). There have been several reports on what the limit of bacterial growth could be in liquid culture. The maximum *E. coli* cell density reported remains within 175 – 220 g/l dcw (J. Shiloach & Fass, 2005). What are the critical factors to consider when growing a high-density *E. coli* culture? Some of those factors include;

1) O₂ transfer rate: estimation on the amount of O₂ needed per gram of *E. coli* biomass production indicates that there should not be any O₂ limiting effect as long as pure O₂ is used (J. Shiloach & Fass, 2005). Yea-Tyng et al., (1998) reported that avoidance of dissolved oxygen (DO) limitation by increasing the agitation speed or enrichment with pure oxygen can eliminate acetate accumulation. Nevertheless, sufficient O₂ is need for re-oxidizing reducing powers, like NAD(P)H₂ and FADH₂, in the glycolytic pathway. DO level is often a limiting factor to growth rate and protein synthesis, and there is lactate accumulation under O₂-limited growth conditions (Dominguez, Nezondet, Lindley, & Coccagn, 1993; Toyoda, Teramoto, Inui, & Yukawa, 2009). Although O₂ is an essential component in high-density fermentation system, temperature and availability of other nutrients are also crucial in obtaining high-density *E. coli* growth (J Shiloach & Bauer, 1975).

2). the media composition and appropriate concentration of constituents is necessary towards supporting denser *E. coli* growth. Formation of precipitates by media components either through non-soluble divalent metal complexes formation (Dean, 1990) or due to relative concentrations of anions and cations can affect both fermentation and downstream processes (J. Shiloach & Fass, 2005). There is also concern about the osmotic pressure and conductivity resulting from ion concentration in the growth media. According to a report from Winzer and his colleagues, high ion concentration has a detrimental effect on membrane potential and has tendency to activate stress mechanisms that could either interfere with growth rate or completely shut down growth cycle (Winzer, Hardie, & Williams, 2002). As a way of mitigating this media problem, Korz et al., used 80 % feeding solution supplemented with 2 % MgSO₄ and trace elements to achieve 110 g/l dcw in fed-batch fermentation. He reported that higher cell density can be achieved by using glycerol instead of glucose in the feed solution due higher solubility of glycerol (Korz, Rinas, Hellmuth, Sanders, & Deckwer, 1995).

3) acetate accumulation due to excess carbon source, especially glucose, under aerobic conditions (Doelle, Ewings, & Hollywood, 1982). This effect can arise due to rapid growth

on glucose (Bauer, Ben-Bassat, Dawson, de la Puente, & Neway, 1990; el-Mansi & Holms, 1989; Zabriskie & Arcuri, 1986), TCA cycle overloading as a result of fast oxidation through glycolysis (Majewski & Domach, 1990), and saturation of electron transport process (Han, Lim, & Hong, 1992). In 1991, Riesenbergr proposed that acetate accumulation could be minimized by feeding glucose slowly into the culture. In this way, TCA cycle can manage every AcCoA produced through glycolysis and cell growth will be reduced (Riesenbergr, 1991). In 1996, Lee proposed an equation (Equation 1) for determining the required feed flow rate to achieve regulated feeding of both glucose and other nutrients into the culture (Lee, 1996).

$$M_S = F(t)S_F(t) = \left(\frac{\mu}{Y_{X/S}} + m\right) X(t)V(t) = \left(\frac{\mu}{Y_{X/S}} + m\right) X(t_0)V(t_0) \exp[\mu(t - t_0)]. \text{ Eq. 1}$$

where; M_S is Mass-flow rate of the carbon source (g/h); F is Feed flow rate (l/h); S_F is Carbon-substrate concentration in the feed (g/l); X is Cell concentration (g/l dcw); m is Specific maintenance coefficient (g/g dcw/h); V is Culture volume (l); t_0 is Time of feeding start; t is Process time; μ is Specific growth rate (l/h); $Y_{X/S}$ is Cell yield on carbon substrate (g/g).

The expression above is based on growth patterns and the expected demand for nutrients; and was derived from well-known average value of *E. coli* yield of glucose (0.5 g/g) and the elemental analysis of *E. coli* cells (C: N: P: S ratio) (J. Shiloach & Fass, 2005). Linear or exponential addition rates of nutrients can be pre-determined using the expression by connecting feed pumps to a controller which estimates the required of carbon needed and adjusts the feed rate accordingly (Lee, 1996; Riesenbergr & Guthke, 1999). On-line monitoring of certain critical fermentation parameters such as pH, dissolved O_2 , CO_2 evolution rate, cell concentration (optical density, NAD, ATP) by feedback control can serve as a feeding system. Also, direct monitoring of concentration of the major carbon substrate can be employed in controlling nutrient feeding into the culture (Korz et al., 1995; Riesenbergr, 1991).

1.4.3. High-Level Expression and Production of Recombinant (Plant) Proteins in *Escherichia coli* by Fed-Batch Fermentation

E. coli strains has continued be the most preferred expression host for production of recombinant proteins due to their well-characterized and readily available genomic information, accessibility of different compatible cloning vectors and expression strains (Sorensen & Mortensen, 2005), fast growth rate and ability to produce high amounts of recombinant proteins at low cost. It also has advantage of biopharmaceutical application because of its FDA-approved status for human use (Ferrer-Miralles, Domingo-Espin, Corchero, Vazquez, & Villaverde, 2009). On the other hand, there has been some limitations to the use *E. coli* host for recombinant production of proteins of eukaryotic origin. This is because of its inability to build disulphide bridges and carryout posttranslational modification. However, it can be conveniently used for production of simple non-modified heterogenous eukaryotic proteins (K. Marisch, K. Bayer, M. Cserjan-Puschmann, M. Luchner, & G. Striedner, 2013).

The central aim of fermentative protein production is to obtain highest possible volumetric yield at lowest cost and shortest time possible (Yee & Blanch, 1992). However, recombinant protein production by fermentation method is often associated with problem of toxic metabolites accumulation which are unfavourable to both cell growth and protein yield. Moreover, the overall productivity of recombinant proteins can be influenced by plasmid stability, promoter response to inducer, post-transcriptional inhibition events, and post-translation inhibition perpetrated by proteolysis and improper folding (J. Shiloach & Fass, 2005). Maintenance of plasmid and its replication consumes a lot of cellular energy. This effect can affect process output as experienced in some plasmid-based expression systems. Furthermore, choice of efficient promoter is crucial for achieving high-level recombinant protein expression. Strong and inducible promoters with low level of basal transcription is often recommended (Karoline Marisch, Karl Bayer, Monika Cserjan-Puschmann, Markus Luchner, & Gerald Striedner, 2013). The common pET system (plasmid for expression by T7 RNA polymerase) has been a good choice in this regard.

Apart from the above-mentioned factors, some factors such as stress response and quorum sensing in *E. coli* influence the yield output of different genes expression or expression using different strains.

1.5. Stability of Recombinant Sugar Beet Hemoglobin

1.5.1. Autoxidation

The association rate and level of stabilization of bound ligands (such as O₂) is quite similar within different classes of nsHbs. Class 1 nsHbs are predominantly pentacoordinated with high O₂ affinities rate constant (R. Arredondo-Peter et al., 1997; Hoy et al., 2007) and high ligand stabilization due to interaction between the bound ligand and the distal histidine (R. Arredondo-Peter et al., 1997).

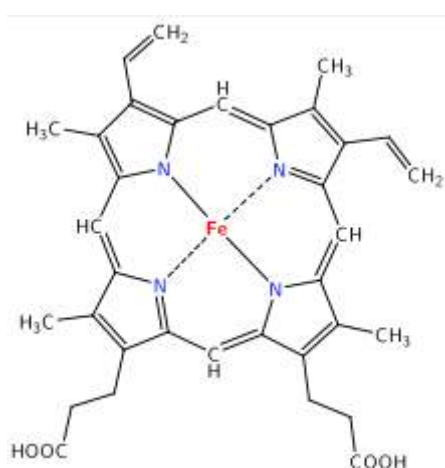
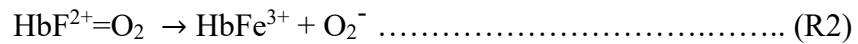
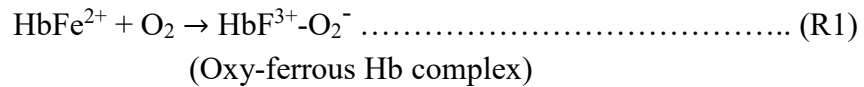


Figure 8. Structure of heme prosthetic group. The heme iron is shown in red and pyrrole nitrogens in blue. Adapted from Wikipedia, The Free Encyclopedia (2017).

As earlier reported, O₂ binds reversibly to the ferrous form of the iron in the heme group (Figure 8). This interaction forms a complex (oxy-ferrous) which exists in form of Fe³⁺-O₂⁻ (R1). When O₂ dissociates, the heme iron returns to Fe²⁺ state. However, O₂⁻ can spontaneously dissociate from the complex leaving the heme iron in oxidized state (Fe³⁺) with resulting superoxide radicals (R2). This process is called autoxidation (Antonini and Brunori, 1971).

Autoxidation occurs in much faster rate in hexacoordinated Hbs compared to pentacoordinated Hbs (Aranda et al., 2009). This is due to the fact that a large “piston” movement of the E-helix along the helical axis is required to move the distal histidine out of the heme pocket for enhanced ligand binding, its positioning as well as stabilization through PheB10 interaction (Smaghe et al., 2009). This is supported by a publication on the sensitivity of autoxidation to changes in the heme ligand binding pocket. Increase in temperature enhances this dynamic changes. Superioxiide ions are produced in the ligand pocket through nucleophilic interaction of bound ligand with distal histidine. At low temperature, these superoxide ions are retained in the pocket but are released as temperature increases to form free radicals and resulting metHbs (R2) (Hochachka, Lutz, Sick, & Rosenthal, 1993).

Apart from hexacoordinate and pentacoordinate properties and temperature, the rate of autoxidation can be influenced as well by presence of solvents (water) and small anions in the heme pocket (Aranda et al., 2009).



2. MATERIALS AND METHODS

2.1. *Bvhb1.1* Cloning and Transformation of Expression plasmid

2.1.1. Cloning of *Bvhb1.1* Gene

2.1.1.1. Amplification and Preparation of pBSK-*Bvhb1.1*

The *Bvhb1.1*-cTP gene with accession number GS54606 was custom synthesized, cloned into SmaI digested pBluescript II SK and delivered as pBSK-*Bvhb1.1* (~100ng/μl) in ddH₂O by Epoch Biolabs. The plasmid (pBSK-*Bvhb1.1*) was transformed into chemically competent *E. coli* TG1 strain (Appendix A1) and plated on LB plates containing ampicillin (100 μg/ml). After incubating overnight at 37 °C using a Termaks incubator (AB Nino Lab., Sweden), a colony was inoculated into LB medium plus ampicillin and grown overnight for plasmid purification. The plasmid was isolated and using the kit (NucleoSpin Plasmid, MACHEREY-NAGEL, Germany); according to the manufacturer's instructions (Appendix A2). The concentration of the purified plasmid was determined by spectrophotometer (Implen Nanophotometer, Labvision AB, Sweden).

2.1.1.2. Subcloning of *Bvhb1.1*

The isolated pBSK-BvHb1.1 was digested with PvuI to cut out the *BvHb1.1* gene. The reaction mix was then separated on Agarose (1%) and the band corresponding to the estimated gene size (2934 bp) was cut and purified using the NucleoSpin Gel Kit (MACHEREY-NAGEL, Germany) (Appendix 5).

All procedures used for subcloning of the purified gene fragment were carried out according to the the Invitrogen Gateway Technology with Clonase II manual (2010-11-07 revised edition). (Appendix A4 and A6). The expression vector used was pDEST42. The expression plasmid (pDEST42-*BvHb1.1*) was purified as previously described, and then sequenced to confirm that the gene sequence and orientation were correct.

2.1.1.3. Transformation of Expression Plasmid

The Inoue method for preparation and transformation of competent *E. coli* BL21(DE3) was used (Appendix A1). The competent cells were transformed with the pDEST42-*Bvhb1.1*, plated on LB plates containing with ampicillin (100 μg/mL) and incubated overnight at 37°C. The plates were stored at +4 °C until use.

2.2. Fed-batch Fermentation and Expression of Recombinant Sugar Beet Hemoglobins

2.2.1. Fed-Batch Fermentation

Each fed-batch fermentation of recombinant sugar beets Hbs was started by cultivating a 30 mL LB supplemented with ampicillin (100 µg/mL). This pre-starter was made by inoculating LB medium with a colony of plated *E. coli*, BL21 (DE3), transformed with any of the recombinant plasmids (pDEST42-*BvHb1.1*, pDEST42-*BvHb1.2* and pDEST42-*BvHb2*). The culture was incubated at 30°C, 100 – 125 rpm for about 9 hours up to OD₆₀₀ 0.5 – 1.0. Thereafter, the pre-starter culture was used to inoculate a fermentation starter prepared with materials listed in Appendix 3. medium containing Davis minimal (DM) broth without dextrose (10.6 mg/mL), L-proline (0.23 mg/mL), metal solution [composed of FeCl₃.6H₂O (27 mg/mL), ZnCl₂ (1.3 mg/mL), CoCl₂.6H₂O (1.27 mg/mL), Na₂.MoO₄.2H₂O (2 mg/mL), CaCl₂.2H₂O (1 mg/mL), CuSO₄.5H₂O (1.27 mg/mL), H₃BO₃ (0.5 mg/mL) and HCl (0.4 M)], and supplemented with Thiamine (30 µg/mL), ampicillin (100 µg/mL), glucose (1 %) and yeast extract (0.2 %) after autoclaving at 121 °C, 1.05 kg/cm² for 20 minutes. The metal solution supplies both the macroelements required for the synthesis of biomolecules (proteins, carbohydrates, lipids and nucleic acids) and the microelements which are needed as cofactors for enzymatic activities. Use of DM broth without dextrose allows use of other substances like Xylose, glucose or glycerol as carbon source during application. The fermentation starter culture was incubated overnight using at conditions as above up to OD₆₀₀ 1.0 – 1.5. Fermentation media, a 3 litre DM culture media prepared with DM broth, L-proline, Metal solution, (concentrations same as in starter media), and Antifoam. Antifoam helps to reduces excessive foam accumulation during cultivation. The DM culture media was transferred into the fermenter (Figure 9A). pH and DO sensors calibrated [for procedure see Appendix A7], inserted into the fermenter and fastened. They all were autoclaved. After autoclaving, the sensors were recalibrated as stated in Appendix 7. Before starting fermentation, the 3 litre DM culture media was completed with Thiamine (50 µg/mL), Carbencillin (100 µg/mL), Glucose (1 %), Yeast extract (0.2 %). Thiamine (Vitamin B1) and yeast extract serves as source of vitamins and other vital nutrients for bacterial growth. Carbencillin provides very stable antibiotic effect under high density cultivation eliminating growth of other bacterial cells. Glucose serves as carbon source to the growing cells. Temperature, pH, and oxygen were set at maximum 30 °C, 6.70, and 40 % respectively. Stirrer speed was initially set at 5 litre/min. and increased gradually depending on glucose and oxygen consumption. Thereafter, it was used to inoculate the prepared fermentor. In all fermentation batches the glucose concentration, optical density at 600 nm (OD₆₀₀) and wet cell weight (wcv) were manually determined and recorded. pH, O₂, and stirrer speed were automatically recorded by the fermenter software, MFC SOPR. Glucose feed (70 %) was supplied into the culture upon glucose depletion at a specific rate set by a feeding profile. The pH was controlled using Ammonium hydroxide (5 M).



Figure 9. 5 L-capacity fermenter. A. A fed-batch recombinant protein fermentation set-up. B. Harvest of cultivated cell culture. A batch is often harvested after 16 – 20 hours of induction.

2.2.2. Expression of Recombinant Sugar Beet Hemoglobins

Protein expression was induced at OD₆₀₀ 25 – 30 with 5 mM δ -aminolevulinic acid (ALA) and 1 mM Isopropyl β -D-1-thiogalactopyranoside (IPTG). The ALA serves as a heme precursor for synthesis of heme. IPTG induces protein expression by binding the *lac*

repressor thereby initiating gene transcription. About 15 minutes before addition of ALA and IPTG, pH, oxygen, temperature, and stirrer speed were set to 6.50, 2 %, 22 °C, and between 3 – 4 lpm (litre per minute), respectively. After induction, the fermentation continued for 16 – 20 hrs. After that, the culture was harvested (Figure 9B). The cells were harvested by centrifugation at 12,000 rpm for 30 minutes. The supernatant was discarded, the recovered cell pellet was resuspended in 10 mM NaP pH 6.0, and again centrifuged. Thereafter, the wet cell weight of pellet was determined and the cells snap-frozen and stored at -80 °C.

2.3. Analysis of Fermentation Sample

2.3.1. Glucose Concentration Measurement

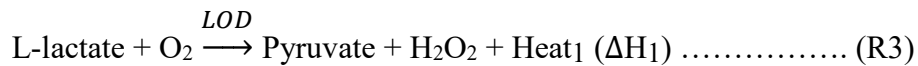
The glucose concentration in the culture was determined with a glucose meter (ACCU-CHEK Aviva, Roche). The procedure was carried out as outlined in Appendix 13. When concentrations were too high, 0.9 % NaCl solution was used to dilute the sample. Saline (0.9 %) was used to avoid cell lysis that could interfere with the measurement.

2.3.2. Wet Cell Weight Determination

To determine wet cell weight (wcw), a 2 mL sample was taken from the fermenter and was centrifuged at 12000 rpm for 10 minutes. The supernatant was stored to be used for lactic acid determination, and the cell pellet recorded in mg/mL. sample name, cultivation date, and time was properly recorded.

2.3.3. Lactic Acid Determination

The assay was carried out using Omics Enzyme Thermistor (Lund, Sweden). This device combines immobilized biocatalysts (enzymes) and heat-sensing elements (thermistors) to measure heat change during enzymatic reaction. A couple of enzymes; Lactate oxidase (LOD) and Catalase, co-immobilized on a packed column oxidizes L-lactate and reduces its intermediate product (H₂O₂), respectively, giving off heat (ΔH₁ and ΔH₂) according to the following equations;



The hydrogen peroxide (H₂O₂) formed from the LOD-catalysed L-lactate oxidation reaction (R3) is reduced to oxygen by catalases which is needed in the reaction and giving off heat (ΔH₂). This process amplified the response obtained which proportional to the concentration of lactate in the sample.

During the assay, standard solutions of 100 mM Lactic acid in 100 mM NaP pH 7.0 buffer were prepared in series of 1 mM, 2 mM, and 4 mM. These standard solutions were used to obtain a standard curve. The same buffer was used as running buffer. After the assay, 20 % Ethanol in 100 mM NaP pH 7.00 was used to clean and store the column. The response obtained was recorded by a computer-controlled potentiometric recorder (in mV), and the sample lactate concentration estimated from the standard curve.

2.4. Extraction and Purification of Recombinant Sugar Beets Hemoglobins

2.4.1. Extraction and Clarification

Cell pellets were resuspended in lysis buffer pH 8.5 (Tris-HCl pH 9.0 (50 mM), NaCl (50 mM), EDTA (1 mM), ascorbic acid (100 μ M), glucose (25 mM), and glycerol (5 %)) and lysed using sonicator QSONICA LLC (Newtown, CT, USA). The Lysis buffer ensures stability, maintain functionality and prevent oxidation of BvHbs. The cell lysed by sonication were clarified by centrifugation at 12,000 rpm for 50 - 60 min. Only in the case of BvHb2 the lysate was bubbled with carbon monoxide (CO) to stabilize the protein. When ion-exchange was going to be used as first purification steps, the cell lysate was overnight dialysed against 50 mM Tris-HCl pH 8.5 using a dialysis membrane from Spectrum Laboratories, US, sample was filtered using 1.2 μ m filter. When hydrophobic interaction was going to be used as a first purification step, the lysate was treated with ammonium sulfate. After centrifugation, the clarified supernatant was filtered using 0.45 μ m syringe filters. Thereafter, samples were loaded onto the correspondent chromatographic column.

2.4.2. Purification

An ÄKTA AVANT system (GE Healthcare), (Fig. 10) was used for all chromatographic separations. All buffers and solutions used for purification process were filtered through 0.45 μ m filter and degassed. Filtration removes any particles, and degassing helps to minimize the formation of air bubbles during the purification process. The runs were carried out at room temperature and the sample was kept on ice. The following chromatographic columns were used for BvHbs purification; Quaternary-sepharose Fast Flow (QFF) strong anion exchanger, Diethylaminoethanol-sepharose Fast Flow (DEAE FF) weak anion exchanger, Butyl-sepharose High Performance (BHP) hydrophobic interaction, Quaternary-sepharose High Performance (QHP) strong anion exchanger and HiLoad Superdex 200 PG gel filtration (GE Healthcare).

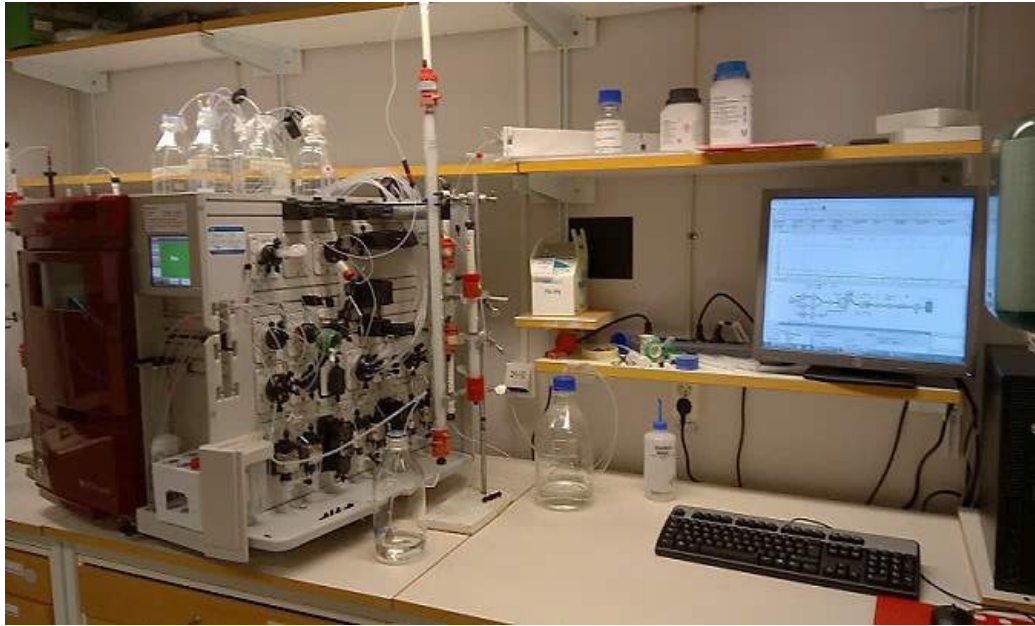


Figure 10. ÄKTA AVANT purification system. The system used for purification processes. The equipment is at Division of Applied Biochemistry, Lund University.

2.4.2.1. BvHb1.1-cTP Purification

QFF strong anion exchange media (with average particle diameter of $\sim 90 \mu\text{m}$) was used for first step purification. The column was equilibrated with start buffer (50 mM Tris-HCl pH 8.5). Target conductivity of the start buffer was 1.1 – 1.4 mS/cm and 3.0 – 4.0 mS/cm during sample application. This is to achieve maximum adsorption of the target protein to the media. The target protein was eluted by increasing salt strength and conductivity using Tris-HCl 50mM + NaCl 200 mM pH 8.5 as the elution buffer. Re-equilibration of the column was carried out using 1 M NaCl and double deionized (dd) water. Eluted protein fractions were concentrated using Vivaspin Protein concentrators (10,000 MWCO) from Sartorius Biotech, frozen in liquid nitrogen and then stored at -80°C until next purification step.

The second step purification of the protein was done using a hydrophobic interaction column, BHP. This media has average particle diameter of $\sim 34 \mu\text{m}$ that provides high removal of bulk impurities. During sample preparation, protein solution was thawed on ice and treated with saturated Ammonium sulphate solution to precipitate out other contaminating proteins in the sample. The saturated Ammonium sulphate was added up to 1.6 M (40 %) concentration in the sample. The estimated volume of the saturated Ammonium sulphate solution was slowly added into the protein solution and stirred for 20 min. The sample was then centrifuged for 10 min. at 1500 rpm. The recovered supernatant was filtered with $1.2 \mu\text{m}$ filter. The column was equilibrated with start buffer (Tris-HCl 50 mM + $(\text{NH}_4)_2\text{SO}_4$ 1.5 M pH 8.5). Target conductivity was 175 – 176 mS/cm. After binding, the protein was eluted with the elution buffer (50 mM Tris-HCl pH 8.5), and column re-equilibrated with dd water for next run. The protein was concentrated and stored as above described.

For the third purification step, QHP strong anion exchange media (particle diameter of ~34 μm) was used. The start and elution buffers used were; 50 mM Tris-HCl pH 8.5 and Tris-HCl 50 mM + 0.1 M NaCl pH 8.5, respectively. After sample binding, the target protein elution was eluted by gradient.

Lastly, the protein was further polished using a Hiload Superdex 200 PG gel filtration column. NaP 50 mM + NaCl 150 mM pH 7.2 was used both for column equilibration and target protein elution. The eluted target protein was concentrated and stored as above.

2.4.2.2. BvHb1.2 Purification

BvHb1.2 was also purified in four steps. In the first step, the crude lysate dialysed dialysed against 50 mM Tris-HCl pH 8.5 buffer and filtered using 1.2 μm . Then it was loaded onto a QFF strong anion exchange column (same as used for BvHb1.1) equilibrated with 50 mM Tris-HCl pH 8.5 buffer. Target protein elution was performed using Tris-HCl 50 mM + 0.2 M NaCl pH 8.5. Eluted fractions were concentrated with Vivaspin Protein concentrator and stored at -80 °C until next step run.

The second purification step was carried out using BHP hydrophobic interaction. Saturated ammonium sulphate solution was added to the protein solution up to 1.4 M (35 %) concentration. After ammonium sulfate addition the protein was stirred for 20 min. The sample was then centrifuged for 10 min. at 1500 rpm. The supernatant was recovered and filtered with 1.2 μm syringe filter. Before sample application onto the BHP column, the column was equilibrated with a mixture of 90 % start buffer (Tris-HCl 50 mM + $(\text{NH}_4)_2\text{SO}_4$ 1.5 M pH 8.5) and 10 % elution buffer (50 mM Tris-HCl pH 8.5) to have approx. the same ammonium sulphate concentration in both the sample and on the column. The conductivity obtained was 159 – 161 mS/cm. Target protein elution was achieved by gradient elution reducing the salt concentration. Column re-equilibrated was carried out with dd water for next run.

QHP strong anion exchange was used on the third step purification step. The protein solution obtained from BHP purification was dialyzed overnight against 50 mM Tris-HCl pH 8.5. The start and elution buffers used were; 50 mM Tris-HCl pH 8.5 and Tris-HCl 50 mM + 0.1 M NaCl pH 8.5, respectively. The target protein was eluted by gradient elution by increasing salt concentration.

The final step used for BvHb1.2 purification was gel filtration method. The process was the same as described for BvHb1.1 Eluted fractions were concentrated and stored as previously described.

2.4.2.3. BvHb2 Purification

Slightly new methods were used in BvHb2 purification including a trial method aimed to remove as many contaminating proteins in the crude lysate as possible. In one of the methods, BvHb2 crude lysate was loaded to a DEAE FF column. The media is a weak anion exchanger with beads of about 90 µm diameter. All purification conditions, buffers and solutions used were the same as those used with QFF.

BHP hydrophobic interaction was subsequently used. Saturated ammonium sulphate solution was added to up to 1.5 M (37.5 %) concentration. The estimated volume of saturated ammonium sulphate solution was slowly added into the protein solution sample and stirred continuously for 20 min. The sample was then centrifuged for 10 min. at 1500 rpm. The supernatant was recovered and filtered with 1.2 µm syringe filter. The column was equilibrated with start buffer (Tris-HCl 50 mM + (NH₄)₂SO₄ 1.5 M pH 8.5) trying to reach a conductivity of 175 – 176 mS/cm. Gradient elution by decreasing the salt concentration was used to elute the protein. The concentrated eluted protein was run on SDS-PAGE and since the result showed that the protein wasn't pure enough an alternative method was tested.

In this alternative method ammonium sulphate powder was added to the crude lysate up to 1.5 M concentration in three consecutive steps of 0.5 M each. At each step, solid ammonium after solid ammonium sulphate was added the sample was stirred for 20 minutes and centrifuged at 12000 rpm for 30 minutes. Thereafter, the 1.5 M ammonium sulphate crude lysate was filtered using 0.45 µm filters. Afterwards, BHP column was equilibrated with start buffer (Tris-HCl 50 mM + (NH₄)₂SO₄ 1.5 M pH 8.5) and the target protein eluted with the elution buffer (50 mM Tris-HCl pH 8.5).

The two batches of BvHb2 purified on BHP column were separately on QHP column. The same procedure and conditions, from dialysis to protein concentration and storage, as with BvHb1.1 was followed. Gel filtration was again used as before to polish the target protein. The eluted sample was concentrated and stored as described above.

2.4.3. Gel Electrophoresis of Sugar Beet Hemoglobins

The purity of BvHbs was evaluated by sodium dodecyl sulphate polyacrylamide gel electrophoresis (SDS-PAGE) after each purification step. Protein samples were mixed with 2× SDS dye and heated for 6 minutes on a 98 °C heat block. Thereafter, the samples and protein ladder (code #: 26614, from ThermoScientific, Lithuania) were loaded into a Mini-PROTEAN precast gel (Bio-rad, USA). The gel electrophoresis was run at 100 Volts, for 70 minutes. At the end of the run, the gel was stained with a solution of 0.1 % Coomassie Brilliant Blue R-250 in 50 % Methanol + 10 % Ethanoic acid (Hochachka et al.) for 1 hour, for protein pattern visualization in the gel. The excess dye was destained in 50 % Methanol + 10 % Ethanoic acid + 40 % dd water destaining solution to remove excess dye. PAGE gel image visualization was performed using Stain-free enabled Gel Doc XR+ imaging system (from Bio-rad, Japan) and analysed using Quantity One 1-D analysis software (from Bio-rad).

2.5. Quantification of Hemoglobin and Heme Concentrations

2.5.1. Hemoglobin Quantification:

The concentration of Hb in the samples were determined by spectroscopy (UV-Vis spectrophotometer Agilent Cary 60) using its carboxy-form of Hb (CO-Hb). To obtain this, protein sample was treated with a few grains of NaD to reduce any oxidized Hb and deoxygenate any oxy-Hb. Thereafter, CO was bubbled into the sample and absorbance spectra measured. The amount of Hb (in mg) was quantified as shown in equation 3.

$$A = \epsilon Cl \dots\dots\dots \text{Eq. 2}$$

$$\text{Conc. (mg/ml)} = \frac{A \times \text{Mwt.} \times \text{Vol.}}{\epsilon} \dots\dots\dots \text{Eq. 3}$$

where A is absorbance, ϵ is extinction coefficient (mM⁻¹.cm⁻¹), C is concentration (in mM), l is path length of beam of light through the sample, Mwt. is molecular weight of the protein, and vol. is volume of sample. The extinction coefficient, ϵ , [Appendix 9] used to calculate the concentration of each BvHbs was determined in-house.

To estimate the amount of Hb produced per litre cell culture and per gram of cell, the result obtained from equation 2 was divided by the total volume of the culture and the gram weight of the cell pallet used, respectively.

Real absorbance of crude lysate Hb was estimated by 3-point drop method expressed in equation 5 below. This method ensures baseline adjustment and eliminates possible interference of other components of the sample that could absorb at the same wavelength as haemoglobin.

$$\text{Real Abs} = \text{Max. peak (c)} - \frac{a - b}{2} \dots\dots\dots \text{Eq. 4}$$

where maximum peak is the absorbance at maximum peak, a and b are the absorbance at points indicated in Figure 11.

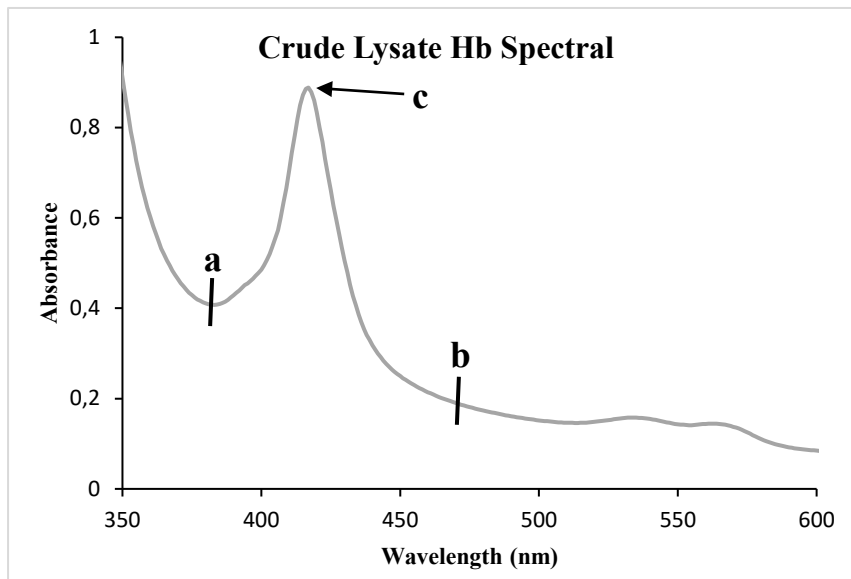


Figure 11. Spectrophotometric absorption spectra of crude lysate CO-BvHb. The plot shows where the values used for the 3-point drop method for crude lysate Hb real absorbance determination were obtained on a given spectrum.

2.5.2. Quantification of Heme Concentration

Pyridine hemochromagen method was used to determine total heme concentration in protein solution [A]. This method involves complete conversion of all heme present in the protein solution into complex with pyridine under alkali condition and subsequently reduction of the heme iron-pyridine complex prior to spectrophotometric measurement [Antonini E. and Brunori M., 1971].

During the assay, a mixture of NaOH (100 mM), Pyridine (20 %), water and then the sample were prepared in a 1.5 ml quartz cuvette. The volume of the sample used and water added depends on the concentration of Hb in the protein solution. The mixture was incubated for 3 – 5 minutes, and thereafter used to obtain baseline within 500 – 600 nm using Cary 60 UV-Vis spectrophotometer (Agilent Inc., USA). Few grains of solid Na₂S₂O₄ powder was added into the mixture and incubated again for 3 - 5 minutes after which the absorbance spectrum was measured. The NaOH serves to maintain the stability of sodium dithionite, pyridine serves as a ligand for heme iron in the reduced state, and Na₂S₂O₄ was added to reduce oxidized heme iron from ferric (+3) to ferrous (+2) state [Barr I. and Guo F, 2015]. The total heme concentration (in millimolar) was determined substituting values obtained from figure 2-4 into equation 5; and the amount (in mg/mL) calculated using equation 3.

$$\left[\left(\frac{[\text{Highest peak } (\sim 555 \text{ nm}) - \text{Lowest point } (\sim 539 \text{ nm})]}{20.7} \right) \times \text{Dilution factor} \right] \dots\dots\dots (5)$$

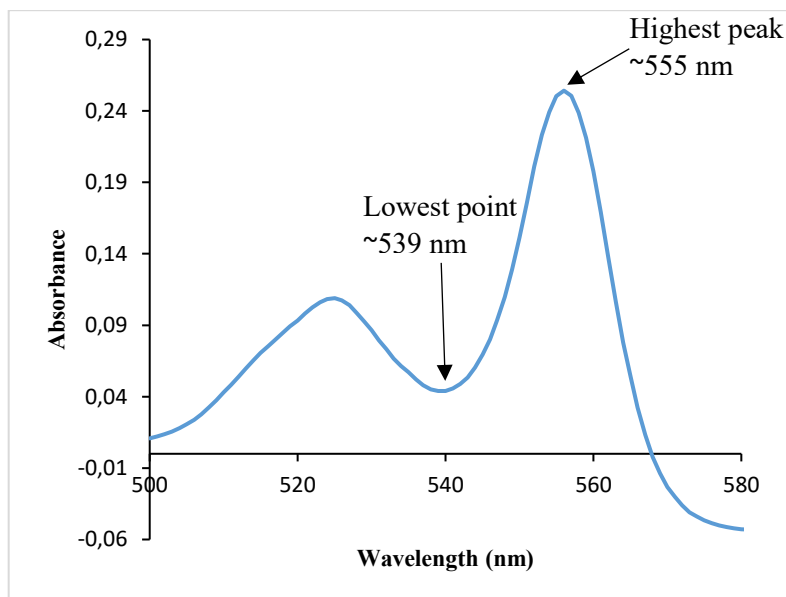


Figure 12. Heme spectrophotometric spectra. The spectral of a reduced heme iron. The points used for estimating heme concentration of a given BvHb sample is indicated by arrows.

2.6. Stability Assay: Autoxidation

Protein Sample Preparation

Protein sample was treated with NaD powder and mixed thoroughly by pipetting up and down. $\text{Na}_2\text{S}_2\text{O}_4$ was added to reduce any oxidized heme iron in the protein sample and deoxygenate oxy-Hb form. The sample was transferred onto PD-10 desalting column (from GE Healthcare, Uppsala, Sweden) equilibrated with 100 mM Na_2SO_4 pH 7.00 buffer. PD-10 desalting column (composed of Sephadex G-25 medium) works on the same principle as gel filtration which separates molecules based on their size differences. The deoxygenated ferrous Hb picks up oxygen from the buffer during elution and become oxygenated. After sample elution, heme concentration of the eluted sample was determined and used to estimate the volume required for autoxidation assay. A thin layer of mineral oil was used to cover two out of three replicates of the sample surface before spectrophotometric measurement. The oil on top of the sample helps to prevent sample evaporation.

Spectrophotometric measurement

The prepared protein sample was run on Cary 60 UV-Vis spectrophotometer using kinetic spectra program that measure absorbance spectra changes at a given time interval. Two-cycle stages were run each at 37 °C and 20 °C for 5 hrs. and 60 hrs., respectively, as presented in table 1.

Table 1. Number of cycles and time for spectral autoxidation assay.

Stage	37 °C		20 °C	
	Cycle (minutes)	Stop (minutes)	Cycle (minutes)	Stop (minutes)
1	5.0	60.0	15.0	120.0
2	20.0	300.0	30.0	3600.0

At the end of the run, the samples were treated with 50 mM Potassium ferricyanide (KFCN) to confirm complete oxidation.

3.0. RESULT

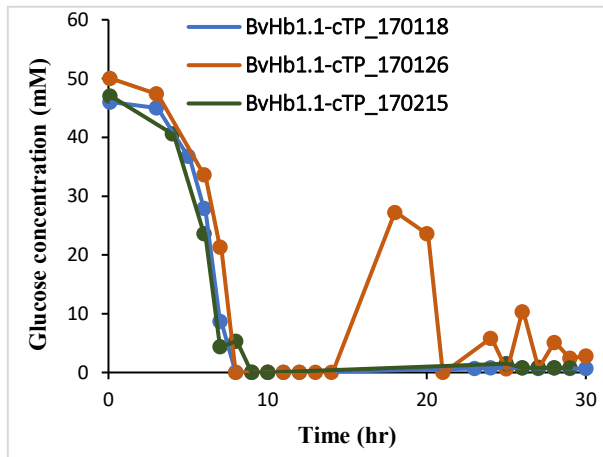
3.1. Fed-Batch Fermentation

3.1.1. Fermentation Data Analysis

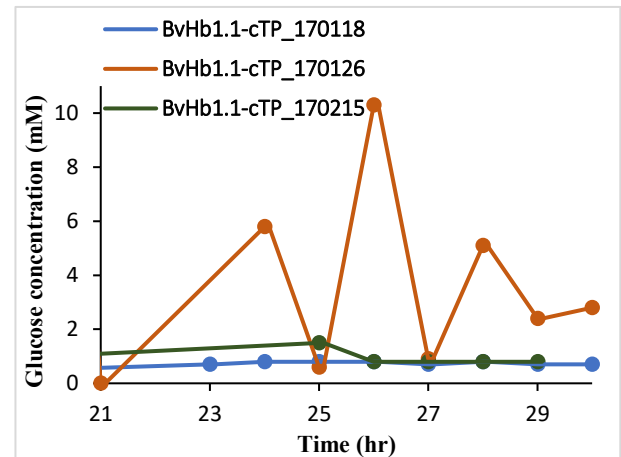
3.1.1.1. BvHb1.1-cTP Fermentation Data Analysis

Three fermentation batches of BvHb1.1 were made, each labelled with its date of cultivation: BvHb1.1_170118, BvHb1.1_170126, and BvHb1.1_170215. During the experiment, two critical parameters (Glucose concentration and Aeration rate) were varied in the first two batches. The data obtained was used to optimize the third batch. As reference, the in-house established procedure for human Hb fermentation was used (Appendix: A11). Figure 13 shows the analysis of the five selected parameters across the three-batch fermentation of BvHb1.1

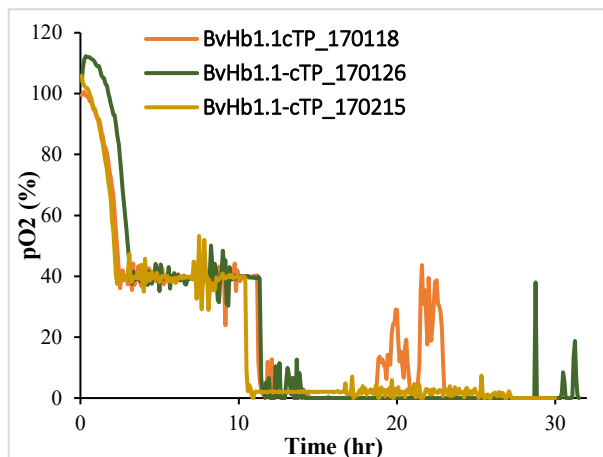
A. Glucose concentration



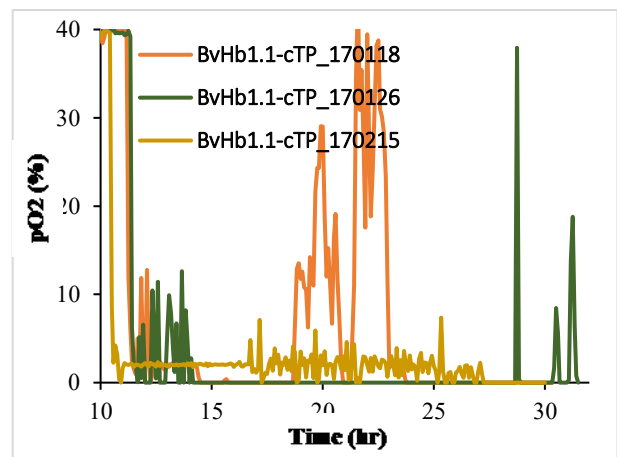
A2. Glucose concentration (enlarged)



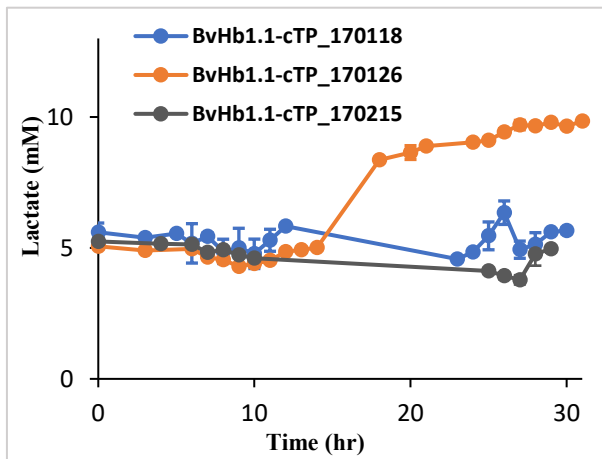
B. Oxygen pressure saturation level



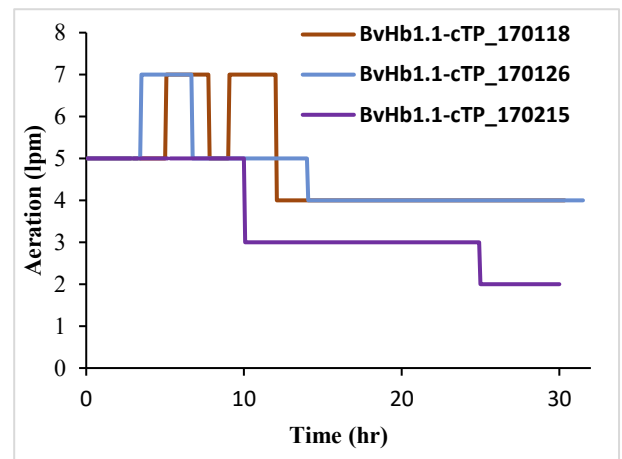
B2. Oxygen pressure saturation level



C. Lactate



D. Aeration rate



E. pH

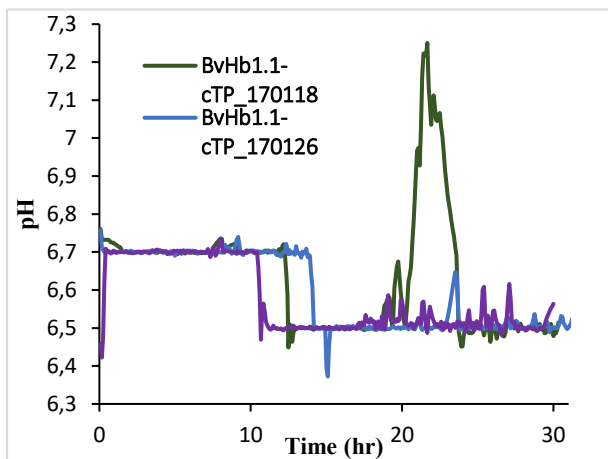


Figure 13. Variations of five fermentation parameters (Glucose concentration, pO_2 , lactate, aeration, and pH) in BvHb1.1-cTP fermentation. pO_2 , aeration and pH data were obtained on-line, whereas Glucose and lactate concentrations were obtained off-line. The lactate data is presented as mean lactate concentration \pm SD. All batch fermentations were started with 100 % O_2 saturation and culture glucose concentration of 50 gL^{-1} .

When the first two batches were analysed, a sudden increase in O₂ saturation (Figure 13B2) and pH (Figure 13E) were observed between 18 and 22 hours. Within this time interval, no base consumption was observed (data not shown). Unfortunately, no culture glucose concentration record was obtained during this period to ascertain glucose level because this was during overnight cultivation. In the second batch (BvHb1.1_170126) aeration rate was varied and glucose feeding profile modified based on the overall result from the first batch. From the data obtained, zero O₂ saturation level was observed from about 14 hours (Figure 13D). Also, high glucose concentration was measured from cell culture (Figure 13A, A2) as well as increase in lactate concentration (Figure 13C). Although pH data showed relatively normal pH level, we observed very high base consumption (data not shown). This confirms that there has been high secretion of lactic acid in the cell culture. With the information obtained from both batches, the third batch was cultivated with a modified glucose feeding profile and aeration rate with aim of optimizing fermentation conditions. Interestingly, the fermentation data showed great improvement in all parameters that were monitored. Specifically, figures 13A, 13B2, and 13C show minimal glucose concentration in the media, quite normal O₂ saturation level, and low lactate secretion.

3.1.1.2. BvHb1.2 Fermentation Data Analysis

BvHb1.2 was cultivated in three different batches (BvHb1.2_160906, BvHb1.2_161109, and BvHb1.2_170220). As with BvHb1.1, five fermentation parameters (Glucose concentration, aeration rate, lactate, pH, and O₂ saturation level) were monitored and the results obtained from the first two batches was used to optimize conditions in the third batch. In this case, the human Hb fermentation was also used as reference. In the result obtained from the first fermentation batch, a rapid increase in culture glucose concentration was measured at about 10 hours (Figure 14C). There was also a corresponding increase in lactate concentration (Figure 14C). An increase in aeration rate from 7 lpm to 10 lpm (Figure 14B) resulted in increase in pH level (Figure 14D) and a slight increase in lactate concentration. The second batch was cultivated with a modified glucose feed profile and aeration rate. From figure 14C, zero O₂ saturation level was recorded in the culture at about 10 hours. There was also an increase in both glucose (Figure 14A) and lactate concentration (Figure 14C). Also the pH increased to 6.90 (Figure 14D). No glucose or lactate data was obtained within this period, but on-line base consumption data showed no base consumption within this time. Although aeration rate was reduced from 4 lpm to 3 lpm (Figure 14B) with some manual addition of glucose feed, a consistent increase in culture O₂ saturation level was notice (Figure 14E2) as well as lactate concentration. The third batch was cultivated at lower aeration rates (Figure 14B) and using the same glucose feed profile as in first batch (Appendix; A11). As expected, there was overall improvement in all the fermentation parameters monitored. However, zero O₂ level (Figure 14E2) as well as increase in lactate concentration (Figure 14C) was observed towards the end of the fermentation. These changes correspond to when aeration rate was dropped from 3 lpm to 2 lpm (Figure 14B).

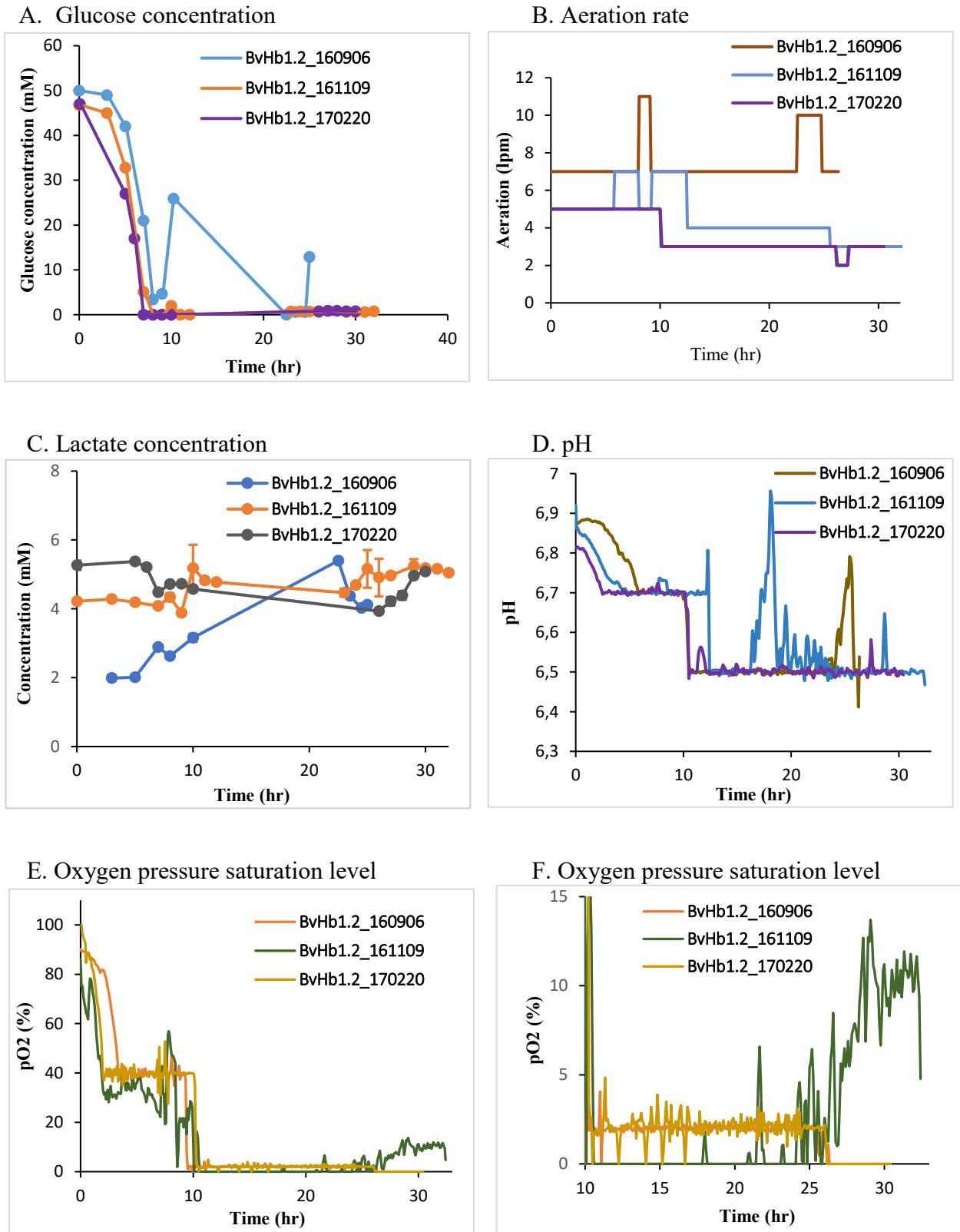


Figure 14. Variations of five fermentation parameters (Glucose concentration, pO₂, lactate, aeration, and pH) in BvHb1.2 fermentation. pO₂, aeration and pH data were obtained on-line, whereas glucose and lactate concentrations were obtained off-line. The lactate data is presented as mean lactate concentration \pm SD. All batch fermentations were started with 100 % O₂ saturation and culture glucose concentration of 50 gL⁻¹.

3.1.1.3. BvHb2 Fermentation Data Analysis

Three fermentation batches were also cultivated with BvHb2. Figure 15 shows plots of analysed data of the five critical fermentation parameters monitored. Those parameters include; glucose concentration, aeration, lactate concentration, pH, and O₂ saturation level. All batch parameters are labeled with date of fermentation. The first batch was cultivated is BvHb2_161025. The result obtained from analysed data from this batch indicated 3.4 mM and 4.7 mM glucose in the culture at 12 hours and 22 hours, respectively (Figure 15A), a fluctuating of pH between 6.50 and 6.60 within this period (Figure 15D), and a slight increase in lactate concentration (Figure 15C). Increase of the pH under high glucose concentration and fermentative condition is an indication of by-product secretion; pH increase arises from ethanol secretion and the measured increase of lactate concentration showed secretion of lactate. The second batch (BvHb2_161104) was cultivated using modified glucose feeding profile (Appendix: 11A) and lower adjusted aeration rate. The analysed batch data showed slightly higher dissolved O₂ (up to 4.2 %, the set point was 2 %) (Figure 15E2), higher lactate secretion (Figure 15C) and higher pH (Figure 15D) after induction that what was observed in the first batch. Higher lactate concentration was already measured at 0 hour of cultivation at this second batch, implying that lactate secretion was already high in the pre-start and/ or starter culture. The high pH fluctuating occurred when no glucose concentration was measured, but O₂ saturation on-line data showed fluctuation was. Glucose concentration was measured later to be 1.2 mM which is relatively high (Figure 15A). This indicates that the high glucose in the culture resulted in the secretion of by-products and pH fluctuations. With the results obtained from the first and second batch, we intended to optimize the third batch by using same glucose feeding profile as in first batch and reducing further aeration rate. Data analysed at the end of the fermentation showed that one of the selected conditions, reduction of air flow rate, was not favourable. From figure 15E2, we observed that there was no dissolved O₂ in the culture after reducing the aeration rate from 5 to 3 lpm (Figure 15B). When increased back to 5 lpm, dissolved O₂ increased very rapidly and the set point of 2 % could not be attain. Our data also showed that there was high glucose concentration within this period (Figure 15A). There seems to be only slight effect on lactate secretion as high lactate concentration analysed in the batch (Figure 15C) came from the starter culture. Plot of on-line obtained pH data (Figure 15D) showed almost normal pH level. This is not surprising because it correlates with the base consumption on-line data obtained (data not shown) which shows high base consumption during this period. This means that the fermentation process was under anaerobic condition and that a lot of base has been used to maintain pH level. It can also be stated that the observed high glucose concentration in the culture at zero dissolved O₂ was the result of low metabolic rate in the cells.

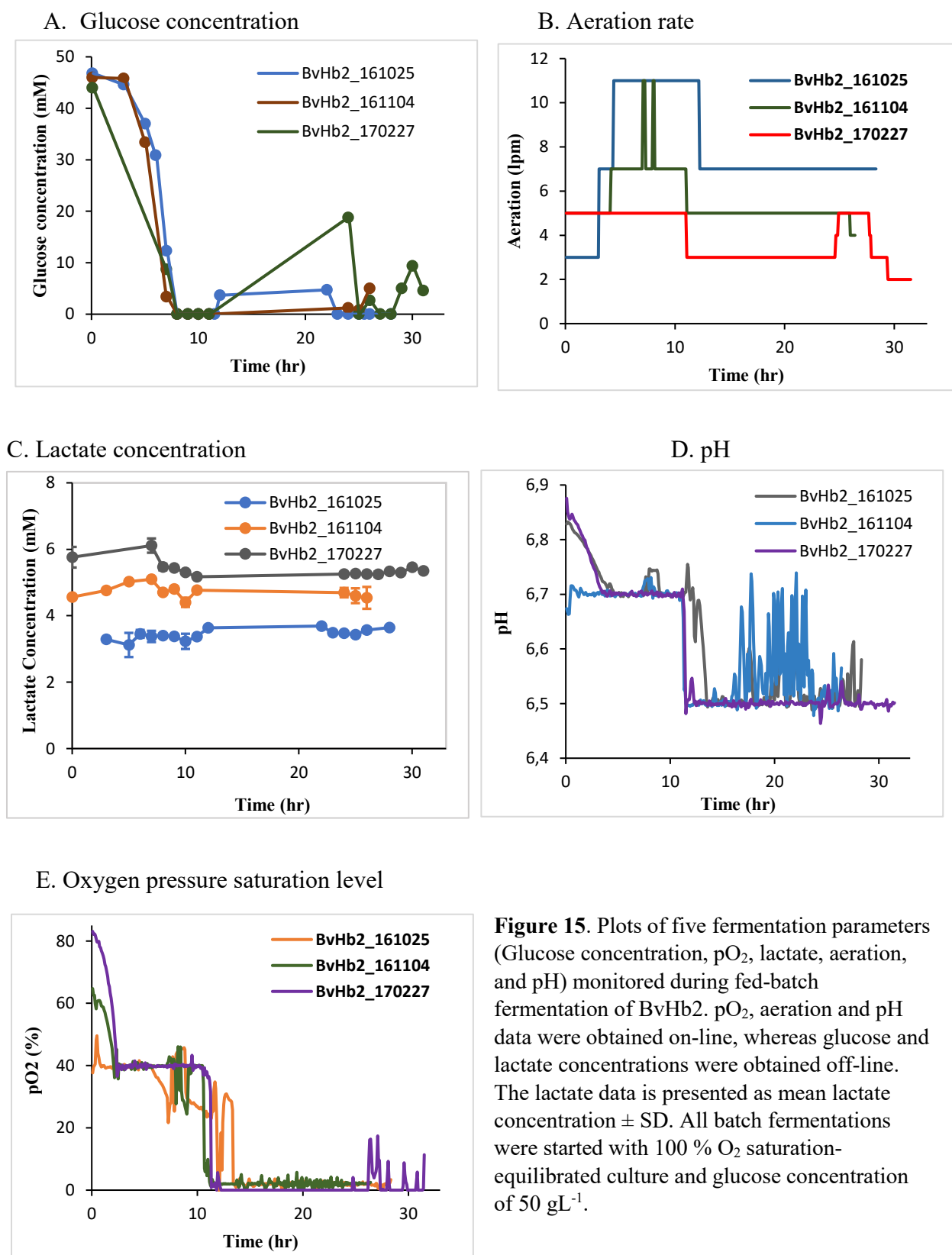


Figure 15. Plots of five fermentation parameters (Glucose concentration, pO₂, lactate, aeration, and pH) monitored during fed-batch fermentation of BvHb2. pO₂, aeration and pH data were obtained on-line, whereas glucose and lactate concentrations were obtained off-line. The lactate data is presented as mean lactate concentration ± SD. All batch fermentations were started with 100 % O₂ saturation-equilibrated culture and glucose concentration of 50 gL⁻¹.

3.1.2. Batch Hemoglobin Yield Analysis

The fermentation output (cell density produced and Hb expression yield) was estimated for all cultivated batches (Table 1). Wet weight of cell pellets were used to estimate cell density in g/L w/w (Figure 16). A defined amount of cell pellet was sonicated and the concentration of Hb from the clarified crude cell lysate used to estimate expression yield by spectra absorption method (Eqns. 2 and 3). Expression yield of each fermentation batch is an important factor when analysing batch fermentation and its optimization. In the BvHb1.1 fermentation, cell densities (g/L w/w) of 178.0, 91.36, and 144.61 were obtained for the first, second, and third batches, respectively. The estimated Hb yield per g cell (mgHb/g cell) for the three batches was, 0.83, 0.73, and 1.15, respectively (Table 1). Although the cultivated cell density was higher in the first batch (178.00 g/L w/w) compare to the third batch (144.61 g/L w/w), the overall expression yield in the third batch (1.15 mgHb/g cell) was about two-fold the first batch (0.83 mgHb/g cell). This result confirms high improvement in the third fermentation batch as observed in the fermentation parameters.

Expression yield and cell density produced in BvHb1.2 fermentation did not show a direct correlation. As tabulated in table 3-1, the first batch produced a cell density of 158.49 g/L w/w and Hb yield of 1.87 mgHb/g cell, second batch produced a cell density of 206.49 g/L w/w with a Hb yield of 1.60 mgHb/g cell, and the third batch cultivated under optimized conditions produced 161.76 g/L w/w and an expression yield of 2.34 mgHb/g cell. Our fermentation data analysis (Figure 3-3) showed overall best fermentation conditions in the third batch. And this is confirmed by the highest expression yield obtained from this batch. Even though the cell density obtained was not the best, it can be inferred that the fermentation conditions used was most favourable for this protein expression. And that it met our target of producing highest possible product.

The BvHb2 fermentation output showed different trend than the other two proteins. From table 1, the first batch produced a cell density of 154.68 g/L w/w with Hb expression yield of 0.37 mgHb/g cell, respectively. The second and third produced cell densities of 192.13 and 86.26 g/L w/w with Hb expression yields of 0.89 and 1.55 mgHb/g cell. With the result of monitored fermentation parameters (Figure 3-4), it seems that the first batch had the best fermentation conditions, but the result of expression poor. The third batch considered to have been cultivated under worst conditions, had the best expression yield per gram cell with lowest cell density. This indicates that conditions favourable for cell growth is different from that for protein expression. Our result for BvHb2 fermentation batches implies that the first and the second batches were cultivated under conditions favourable for cell growth while the third batch was cultivated under conditions favourable for Hb expression. Our result on estimated heme yield (Table 2) followed the same pattern as Hb yield. This is expected since heme is a component of Hb molecule.

Table 2. Estimated fermentation output of all batches. The estimated cell densities produced and Hb expression yield were presented.

Cultivated sample Batches	Induction OD600	Wet Wt. of cells produced (g)	Cell Density (g/L wcv)	Estimated Hb yield (mgHb/ L culture)	Estimated Heme yield (mgHb/ L culture)	Estimated Hb yield per g cells (mgHb/g cell)	Estimated Heme yield per g cells (mgHeme/g cell)
170118 BvHb1.1-cTP	32.3	534	178.00	148.26	94.21	0.83	0.53
170126 BvHb1.1-cTP	42.3	274.08	91.36	67.01	53.21	0.73	0.58
170215 BvHb1.1-cTP	25.1	433.84	144.61	166.14	126.04	1.15	0.87
160906 BvHb1.2	31.4	475.48	158.49	297.13	118.40	1.87	0.75
161109 BvHb1.2	35.1	619.47	206.49	329.74	258.23	1.60	1.25
170220 BvHb1.2	29.3	485.272	161.76	378.96	187.73	2.34	1.16
161025 BvHb2	27.2	464.037	154.68	56.86	41.83	0.37	0.27
161104 BvHb2	31.4	576.38	192.13	171.33	141.38	0.89	0.74
170227 BvHb2	27.9	258.78	86.26	134.07	87.07	1.55	1.01

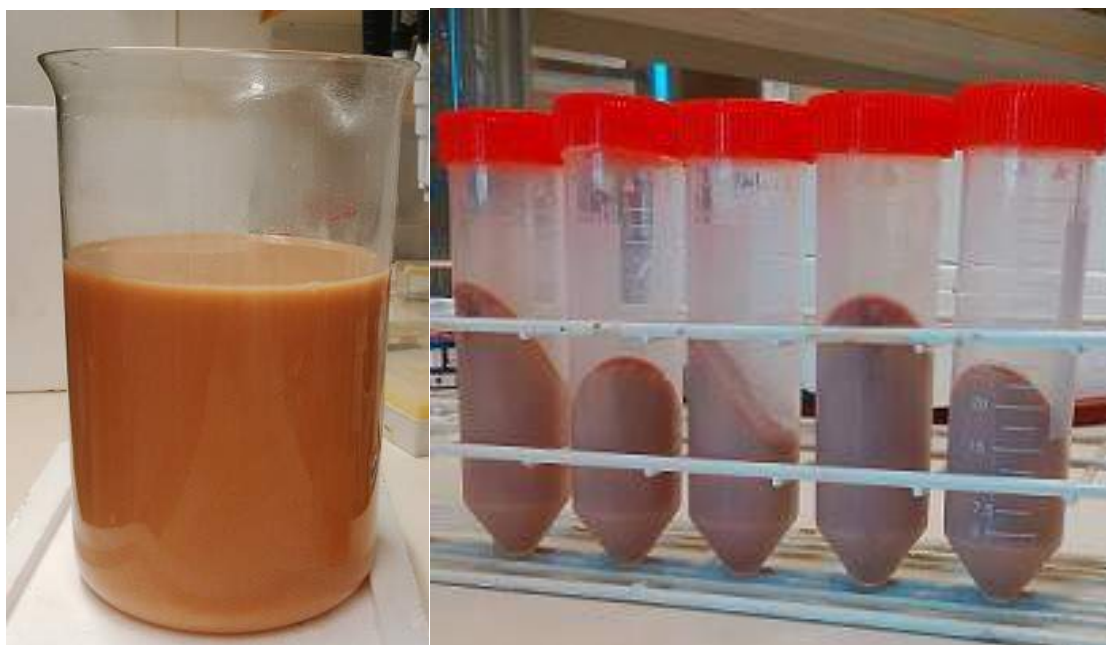


Figure 16. Harvested cell culture (3 litres) and cell pallets. The cell pallets were obtained after centrifuging the harvested culture. Wet weight of the pallets was used to estimate cell density per litre of culture.

Overall yield of each BvHb was calculated as mean \pm SD (Table 3-2). Our result shows Hb yield of around 0.695 – 1.115 mgHb/g cell, 1.568 – 2.308 mgHb/g cell, and 0.348 – 1.528 mgHb/g cell, for BvHb1.1, BvHb1.2, and BvHb2, respectively. This shows that BvHb1.2 expression is the best under the fermentation conditions. This is followed by BvHb2 and then BvHb1.1. Figure 3-6 depicts a plot of the calculated mean \pm SD of all BvHbs expression yield. The error bars indicate yield margin within each BvHb fermentation batches. And the wide difference observed is due to changes in the fermentation parameters used in each batch fermentation. Statistical significant values show $p < 0.05$. This is correct as it implies that the expression levels across the three BvHbs is statistically different.

Table 3. Overall expression yield of BvHbs. Data represent the means \pm SD (n=3) of the three fermentation batches made for each BvHb.

Sample	BvHb1.1-cTP	BvHb1.2	BvHb2
Av. Hb yield/ g cell \pm SD	0.905 \pm 0.21	1.938 \pm 0.37	0.938 \pm 0.59

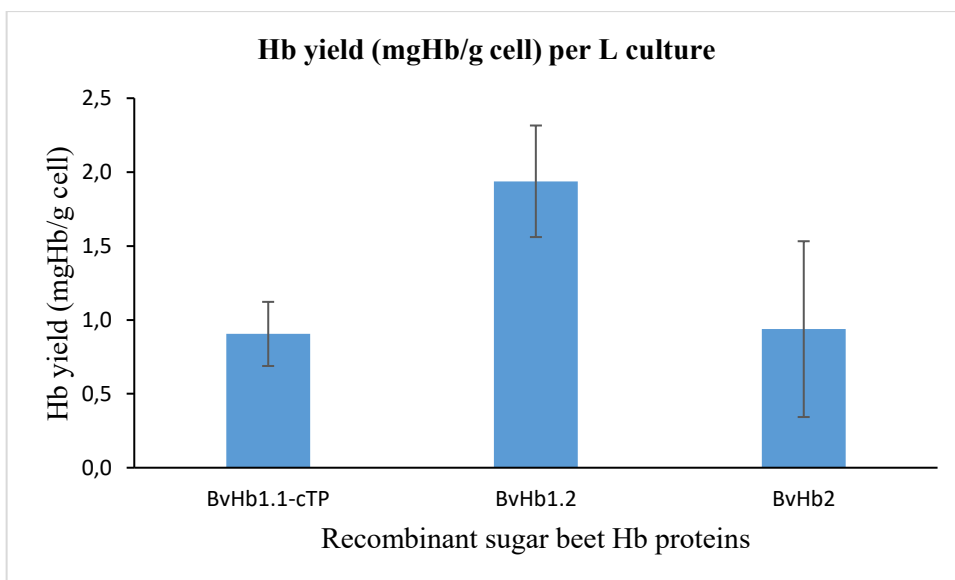


Figure 17. Hb yield mean \pm SD of BvHbs. Data was obtained from estimated crude lysate Hb concentration and analysed using single factor ANOVA. Significant difference $p < 0.05$.

3.2. Sugar Beet Hemoglobins (BvHbs) Purification:

Cell pellets from each BvHb fermentation culture were resuspended in lysis buffer pH 8.5, sonicated and clarified both by centrifugation and filtration. The crude protein lysate obtained was then purified using different chromatographic columns connected to an äkta avant system. Figure 18 depicts concentrated eluted fractions from different purification steps. In figure 10, the SDS-PAGE result of all purification steps is shown. Each band shows the proteins remaining in the sample after a given. In BvHb1.1 purification, few bands were still observed after third purification step with QHP. After purifying the sample further on GF column, two bands were left of which one has the expected size (~20 KDa) indicated by the arrow. BvHb1.2 sample shows only one band after fourth purification step. This band correspond exactly to 17.0 kDa expected size. BvHb2 purification was a bit different. SDS gel result shown in figure 19 show many bands that might not be removed on QHP. Consequently, BHP was used as the first purification step instead. The SDS gel result is represented as BHP(T). BHP(T) sample further purified on QHP column showed few bands. When loaded on GF column, two strong bands were still observed. One these bands indicated by arrow correspond to 15 kDa expected gel size of BvHb2.

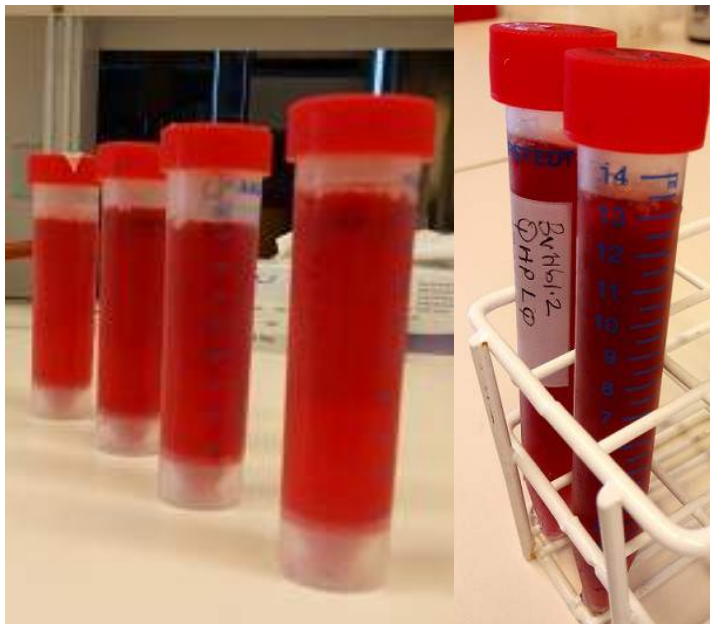


Figure 18. BvHbs after different purification steps. Each of the samples have been purified at a step out of the four steps applied and concentrated.

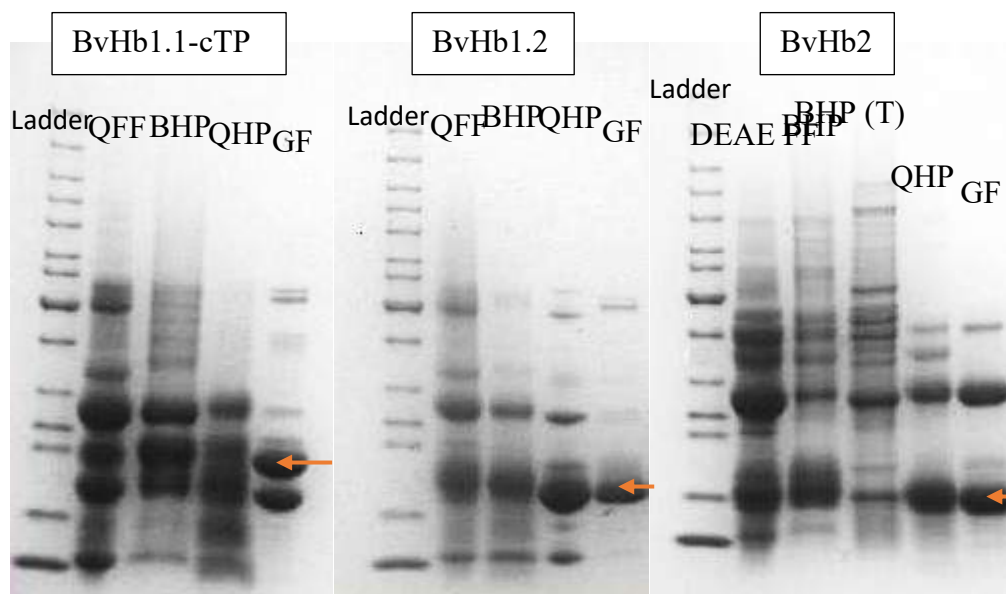


Figure 19. SDS-PAGE result of each purification step. Different purification steps were used, sequentially, to obtain BvHbs in the purest form possible. QFF is Quaternary-sepharose Fast Flow; BHP is Butyl-sepharose High Performance; QHP is Quaternary-sepharose High Performance; GF is Gel Filtration, and DEAE FF is Diethylaminoethanol Fast Flow. BHP (T) represent trial result of using BHP as first purification step. All samples were treated with 2× SDS buffer and run on Bio-rad precast gel. Expected protein sizes are indicated by arrows.

3.3. Autoxidation Assay

Autoxidation assay for BvHb1.2 was carried out using purified sample treated with NaD and separated on PD-10 column. Deoxygenated protein was re-oxygenated during elution with undegassed phosphate buffer. The sample was prepared in three replicates of which two were covered with thin layer of mineral oil (laboratory grade) and the other with parafilm to prevent sample evaporation, and their autoxidation kinetics measured spectrophotometrically. Figure 3-9 shows changes in absorbance spectra during autoxidation of BvHb1.2 in NaP pH 7.0 buffer at 37 °C (Figure 3-9A) and 20 °C (Figure 3-9B); and analysed autoxidation rates at 578 nm for both samples with oil and that without oil layer (Figure 3-9C and Figure 3-9D). This wavelength is one of the points where significant changes occur as shown in appendix A12 for reaction at 37 °C and A13 for reaction at 20 °C. As shown in figures 3-9A and 3-9B, the maximum absorbance spectrum of the sample was obtained at ~411 nm. This corresponds to the established maximum absorption wavelength of oxy-BvHb1.2 (Appendix: A9). The autoxidation rates as estimated from exponential decay plot of the spectra changes at 578 nm from samples with oil and no oil gave, respectively, $5.82 \times 10^{-6} h^{-1}$ and $5.62 \times 10^{-6} h^{-1}$ in reactions at 20 °C (Figure 3-9D). Also, autoxidation rates from spectra changes at 578 nm from samples with oil and no oil were estimated to be $1.64 \times 10^{-4} h^{-1}$ and $2.10 \times 10^{-4} h^{-1}$, respectively, in reactions at 37 °C (Figure 3-9C). Both results show that autoxidation rate is faster at higher temperature, and that, although not the case in reaction at 20 °C, presence of oil film reduces autoxidation rate probably by preventing sample evaporation.

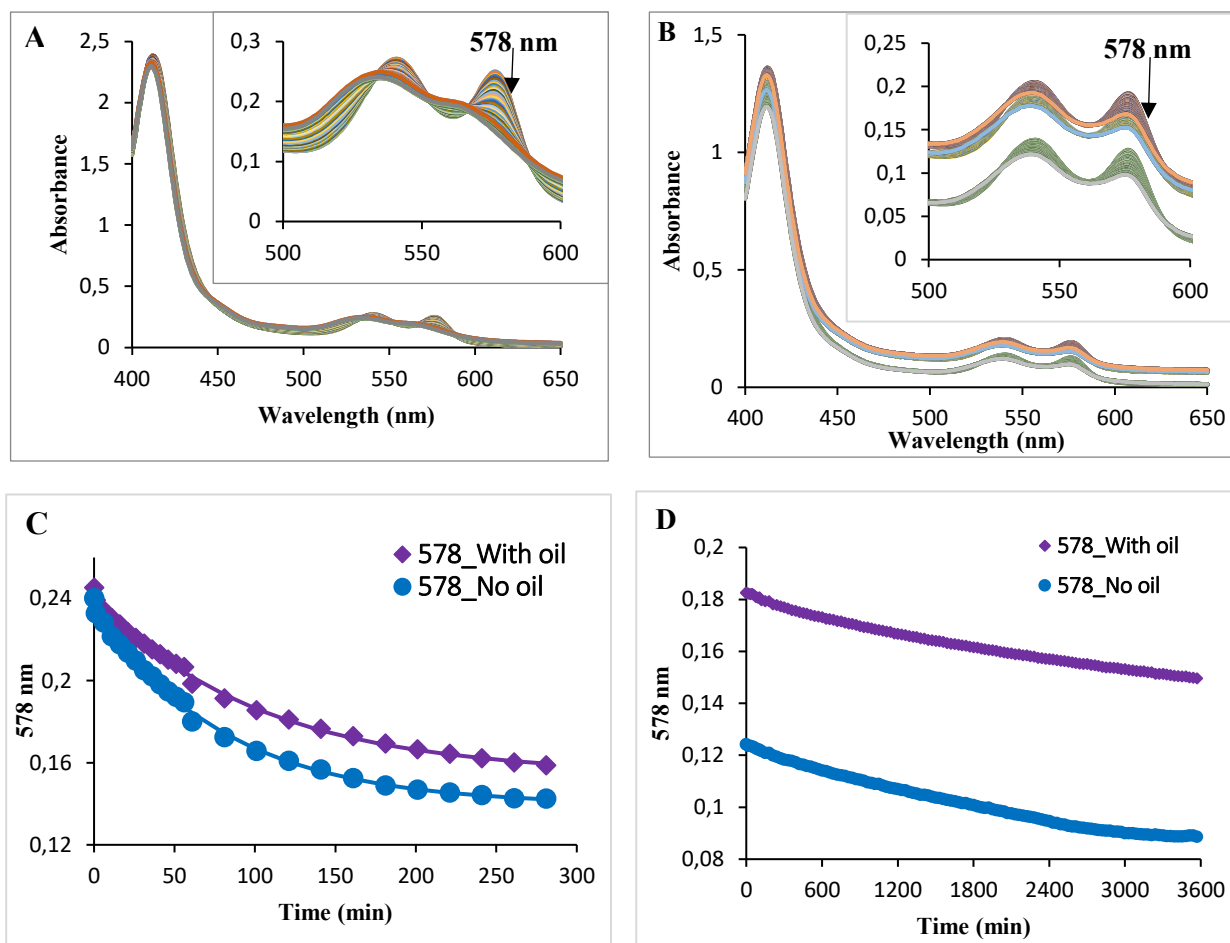


Figure 20. Autoxidation determination of BvHb1.2. Kinetic absorbance spectra for reaction at 37 °C (A) and at 20 °C (B) for both samples with oil film layer and samples with no oil. Autoxidation rate was estimated from the point (578 nm) where significant absorbance change occurred. And exponential decay curve for changes at both temperatures was plotted, respectively, in C and D.

4.0. DISCUSSION

4.1. Fed-Batch Fermentation of Sugar Beet Hemoglobins

Previous work on cultivation of recombinant BvHbs (Eriksson, 2014) has been with traditional shake flask method. This method is only possible with small culture volumes of culture of about 1 L and usually suffer O₂ limitations often towards end of cultivation (Soini, Ukkonen, & Neubauer, 2008). Consequently, fed-batch fermentation technique was designed to reduce cultivation problems associated with O₂ and other nutrients distribution. This technique also provides for efficient on-line monitoring of some critical fermentation parameters making it easier to monitor culture microenvironment conditions.

In this study, we have cultivated recombinant BvHbs each in three batches using a fed-batch fermentation technique. Our intention was to find favourable conditions for fermentation of each of these recombinant proteins. To achieve this, we monitored five critical fermentation parameters of which i.e., glucose concentration, O₂ saturation level, aeration rate, pH, and lactate concentration. Our goal was to make two batches of each of the proteins under similar conditions except glucose feeding profile and aeration rate that were modified. We intended to use results obtained from first two batches to improve third batch.

Earlier studies on glucose metabolism in *E. coli* has shown that glucose metabolism under anaerobic conditions results in the production of different organic acids (acetate, formate, lactate, and succinate), ethanol, carbon dioxide, and hydrogen (Murarka et al., 2010). Our fermentation data analysis result on BvHb1.1-cTP_170126 batch agrees with this report, from the result high lactate concentration was obtained in the presence of high glucose concentration and zero O₂ saturation level (anaerobic condition). On-line base (5 M NH₄OH) consumption data from this batch also shows high consumption of base during this period. This means that a lot of base was used in maintaining pH level under acid secretions. This same effect of high lactate secretion under zero O₂ level was observed in BvHb1.2_170220 and BvHb2_170227 batches. This shows that some level of O₂ is required for glucose fermentation as complete absence of O₂ will result in toxic by-products as observed in the BvHb1.2_161109 batch. BvHb2_161025 fermentation data shows increasing pH level and lactate concentration at high glucose concentration under normal O₂ saturation level (i.e., 2 % set point). A similar effect was also observed in BvHb1.2_160906 where lactate secretion increased under high glucose concentration and sufficient O₂ level. These results agree with earlier findings that fermentation by-products accumulate under sufficient O₂ levels and high glucose concentration due to rapid growth of cells (Bauer et al., 1990; el-Mansi & Holms, 1989; Zabriskie & Arcuri, 1986). High glucose concentration effect can be controlled by use of an appropriate glucose feeding profile that slowly adds glucose into culture (Riesenberg, 1991).

Glucose catabolism yields pyruvate in both aerobic and anaerobic conditions. The route of pyruvate is determined by the prevailing condition of the system. As described by Murarka A et al., (2010), PDHC converts pyruvate to AcCoA, CO₂, and NADH in the presence of oxygen. Under limiting oxygen conditions, the activity of PDHC is replaced by PFL which also converts pyruvate to AcCoA and in addition to formate. The generated

AcCoA is further reduced by both acetaldehyde dehydrogenase (ALDH) and ADH resulting to synthesis of ethanol. According to our result from BvHb1.1-cTP_170118 batch, sudden high fluctuations in O₂ saturation level was accompanied by high pH levels indicating that AcCoA has been produced and converted to ethanol under fluctuating O₂ saturation levels. This observation corresponds with earlier descriptions (Murarka A et al., 2010) on the activities of PDHC, ALDH, and ADH on pyruvate under aerobic and anaerobic conditions. A similar condition was observed in the BvHb1.2_161109 batch where fluctuating high pH levels were noticed under zero O₂ saturation level. This clearly shows ethanol is produced under anaerobic condition. The observed continuous increase in O₂ level even under reduced aeration rate and appropriate glucose concentration could not be related to any known route of glucose metabolism in *E. coli*. However, lactate concentration increase during this period suggests that culture microenvironment is not favourable for O₂ depletion by the cells. Again, from BvHb1.2_160906 batch, we observed that increasing aeration rate few hours before end of the cultivation resulted to increase pH level. High pH level is associated with ethanol secretion and is consequence of anaerobic fermentation. It is possible that a different effect was occurring in the culture when aeration rate was increased as no change was observed with O₂ saturation level.

4.2. Batch Fermentation Output: Cell Density and Hemoglobin Expression Yield

One of the main aims of fermentative recombinant protein production is to achieve optimum productivity (Yee & Blanch, 1992), both in terms of cell density growth as well as in target protein expression level. According to Riesenberget al., (1990), cultivation of *E. coli* cultures is employed in both laboratory and industrial production of recombinant proteins from prokaryotic and eukaryotic origin which are considered to be low-volume-high-value products. This implies that the use of fermentation method in recombinant protein production can give high volumetric yield of low abundant biomolecules. These proteins, BvHbs, are such biomolecules with high economic value but present in very low amounts in *Beta vulgaris ssp. vulgaris*. Therefore, we have used a fed-batch fermentation technique to try to obtain high amounts of these proteins.

Our result in the third batch of BvHb1.1-cTP fermentation showed improvement in both cell density growth and target protein expression yield. Modification of the fermentation parameters especially, glucose concentration and aeration rate has shown to have serious effects on both cell growth and target product accumulation. Similar effects were also observed in both BvHb1.2 and BvHb2 fermentations. As observed, data obtained from these proteins suggest that cell growth and protein expression are influenced by different parameters. This is shown by low estimated protein yield at high cell density. It could be that these proteins expresses under similar conditions as in plant. In 2014, Leiva-Eriksson and her colleagues reported that class 1 nsHbs are expressed at high amounts in germinating seeds and hypocotyl while class 2 nsHbs are expressed at high levels in leaves and flowers (Leiva-Eriksson et al., 2014). It is also established that class 1 nsHbs has high oxygen affinities and low oxygen dissociation rate constants (Kakar et al., 2010). On the other hand, class 2 nsHbs have low oxygen affinities and high oxygen dissociation constants (R. Arredondo-Peter et al., 1997; Hargrove et al., 2000). These effects explains why class 1 nsHb is mainly found in active tissues like germinating seeding and class 2

nsHbs in leaves and flowers where the exchange of gases is very crucial. From our fermentation data results, we observed that almost a double expression yield was obtained in BvHb1.1-cTP when cultivation was carried out under low aeration rate and moderate glucose feeding. A similar effect was also observed in BvHb1.2 fermentation. With this, we conclude that fermentation of class 1 BvHbs requires low aeration rate to supply minimal level of O₂ to the culture. Our result also shows that high glucose concentration in BvHb1.1-cTP and BvHb1.2 fermentations only affected cell growth. This agrees with the report on high expression level of class 1 nsHbs in germinating seeds. Result obtained from cell density and protein expression yield of BvHb2 fermentation could not be compared among the batches, because there are wide differences across cultivation times. This can be perceived from the reported high standard deviation value as well as from error bar obtained from BvHb2 yield analysis. However, it can be proposed from available data that under appropriate glucose levels and other conditions, that high aeration rate seems to be favourable for BvHb2 expression. As it is, more experiments is required to confirm this.

4.3. Purification of Sugar Beet Hemoglobins

Different chromatographic columns comprising of ion exchange, hydrophobic interaction and gel filtration were used to purify the produced recombinant protein. Each purification step was examined by SDS gel electrophoresis to determine their level of purity. Crude lysate clarification and purification is of great concern when considering growing high density cultures. It has been observed that purification of recombinant proteins produced by shake flask cultivation is much easier (with less contaminants) compare to ones produced by fermentation method (Leiva-Eriksson et al., 2014a). In 2005, Shiloach and Fass reported that in addition to antifoam-derived surface agents effect on micro- and ultra-filters, debris from cell lysis is another possible source of impurities that could affect purification processes. Our SDS-PAGE result on different purification stages agrees with this report, that high contaminating impurities are still observed after two purification steps (in BvHb2) and even after three purification steps in BvHb1.1-cTP. This problem is less BvHb1.2 compared to others. Previous work on BvHbs purification has shown that most pure sample can easily be obtained from this protein compared to others (Leiva-Eriksson et al., 2014a). The reason for this remains unknown.

4.4. Autoxidation of BvHb1.2

A process of spontaneous release of O₂ radical from Hb molecule and oxidation of Hb to metHb, is known as autoxidation. Release of O₂ radicals and formation of metHb is temperature dependent, among other things. Free radical formation under increased temperatures result from nucleophilic interaction between the released superoxide ion and heme group distal histidine. This effect is lower at low temperatures because the superoxide ion is tightly kept inside heme pocket (Hochachka et al., 1993).

We determined autoxidation kinetics of BvHb1.2 by using the decrease in spectra absorbance at 578 nm. Our result shows overall increase in autoxidation rate at 37 °C

compared to that at 20 °C. Furthermore, samples covered with oil layer showed lower autoxidation rates compared to the ones without oil. These results agree with earlier reports on the effect of temperature on O₂ dissociation from heme-ligand binding pocket (Hochachka et al., 1993). It was expected that incubation at 37 °C will result to faster destabilization of distal histidine interaction with bound O₂, and thus result to rapid release of superoxide radicals. It also makes sense that samples without an oil layer that was covered with parafilm had faster autoxidation rate due to evaporation effect. Some bubbles were observed under the parafilm which indicates that evaporation had occurred. From our estimated autoxidation rates at 20 °C, we observed that one of the duplicates of samples with oil cover had a higher rate than the one without oil. Our thought is that this could be as a result of human error during sample preparation. This affected our reported value for autoxidation rate at 20 °C as it can be interpreted that rate of autoxidation is faster in samples with thin oil layer cover. It worth to mention that our samples could not complete autoxidation reaction as expected due to machine error. Therefore, we recommend that this assay be repeated to confirm our results.

CONCLUSION

This project was aimed at improving productivity of recombinant BvHbs both by increased *E. coil* cell density cultivation and maximizing BvHbs expression levels. Additionally, we aimed at characterizing the stability of these proteins by studying their autoxidation at different temperatures. We identified that glucose concentration and aeration rate is critical in maintaining favourable conditions for both cell growth and protein expression. The level of fermenter parameters that favour expression differ among the proteins. And this condition seems to be closely related to their expression pattern in the plant. Obtaining these proteins in pure form remains to be a challenge as there seems to be strong interfering substances arising from both fermentation culture components and cell lysis. We observe that temperature had a significant effect in conversion of Hb to metHb, and that the process of autoxidation is very sensitive to structural changes around heme pocket due to temperature-induced dynamic changes.

Although we have identified that culture glucose concentration and level of O₂ saturation is primary in achieving high fermentation outputs, we recommend further experiments to establish if this observation is related to the expression pattern of these proteins. Considering the importance of obtaining these proteins in their purest form, our recommendation is to obtain their crystal structures as well as mass spectrometry data. These will provide more information about tertiary structures of their active forms and chemistry of constituent amino acid residues. It will also be interesting to carry out more stability studies to firmly establish the rate of metHb formation and superoxide ion release across these proteins. With that, comparative studies could be made between plant-based Hbs and already well-studied mammalian-based Hbs for possible use of the earlier in blood substitute development.

REFERENCES

- Alayash, A. I. (2014). Blood Substitutes: Why Haven't We Been More Successful? *Trends Biotechnol*, 32(4), 177-185. doi: 10.1016/j.tibtech.2014.02.006
- Antonini, E., & Brunori, M. (1971). Hemoglobin and myoglobin in their reactions with ligands:[by] Eraldo Antonini and Maurizio Brunori. Amsterdam: North-Holland Pub. Co.
- Aranda, R., Cai, H., Worley, C. E., Levin, E. J., Li, R., Olson, J. S., . . . Richards, M. P. (2009). Structural analysis of fish versus mammalian hemoglobins: effect of the heme pocket environment on autooxidation and heme loss. *Proteins: Structure, Function, and Bioinformatics*, 75(1), 217-230.
- Arredondo-Peter, R., Hargrove, M. S., Moran, J. F., Sarath, G., & Klucas, R. V. (1998). Plant hemoglobins. *Plant Physiology*, 118(4), 1121-1125.
- Arredondo-Peter, R., Hargrove, M. S., Sarath, G., Moran, J. F., Lohrman, J., Olson, J. S., & Klucas, R. V. (1997). Rice hemoglobins. Gene cloning, analysis, and O₂-binding kinetics of a recombinant protein synthesized in *Escherichia coli*. *Plant Physiol*, 115(3), 1259-1266.
- Bauer, K. A., Ben-Bassat, A., Dawson, M., de la Puente, V. T., & Neway, J. O. (1990). Improved expression of human interleukin-2 in high-cell-density fermentor cultures of *Escherichia coli* K-12 by a phosphotransacetylase mutant. *Appl Environ Microbiol*, 56(5), 1296-1302.
- Bren, A., Park, J. O., Towbin, B. D., Dekel, E., Rabinowitz, J. D., & Alon, U. (2016). Glucose becomes one of the worst carbon sources for *E. coli* on poor nitrogen sources due to suboptimal levels of cAMP. *Sci Rep*, 6. doi: 10.1038/srep24834
- Bruno, S., Faggiano, S., Spyraakis, F., Mozzarelli, A., Abbruzzetti, S., Grandi, E., . . . Dominici, P. (2007). The reactivity with CO of AHb1 and AHb2 from *Arabidopsis thaliana* is controlled by the distal HisE7 and internal hydrophobic cavities. *J Am Chem Soc*, 129(10), 2880-2889. doi: 10.1021/ja066638d
- Bunn, H. F., Esham, W. T., & Bull, R. W. (1969). The renal handling of hemoglobin. I. Glomerular filtration. *J Exp Med*, 129(5), 909-923.
- Capece, L., Boechi, L., Perissinotti, L. L., Arroyo-Manez, P., Bikiel, D. E., Smulevich, G., . . . Estrin, D. A. (2013). Small ligand-globin interactions: reviewing lessons derived from computer simulation. *Biochim Biophys Acta*, 1834(9), 1722-1738. doi: 10.1016/j.bbapap.2013.02.038
- Chen, R., Yap, W. M., Postma, P. W., & Bailey, J. E. (1997). Comparative studies of *Escherichia coli* strains using different glucose uptake systems: Metabolism and

energetics. *Biotechnol Bioeng*, 56(5), 583-590. doi: 10.1002/(sici)1097-0290(19971205)56:5<583::aid-bit12>3.0.co;2-d

- Dean, J. (1990). Lange's handbook of chemistry. *Material and manufacturing process*, 5(4), 687-688.
- Doelle, H., Ewings, K., & Hollywood, N. (1982). Regulation of glucose metabolism in bacterial systems. *Microbial Reactions*, 1-35.
- Dominguez, H., Nezondet, C., Lindley, N., & Cocaign, M. (1993). Modified carbon flux during oxygen limited growth of *Corynebacterium glutamicum* and the consequences for amino acid overproduction. *Biotechnology letters*, 15(5), 449-454.
- Dordas, C., Hasinoff, B. B., Igamberdiev, A. U., Manac'h, N., Rivoal, J., & Hill, R. D. (2003). Expression of a stress-induced hemoglobin affects NO levels produced by alfalfa root cultures under hypoxic stress. *Plant J*, 35(6), 763-770.
- el-Mansi, E. M., & Holms, W. H. (1989). Control of carbon flux to acetate excretion during growth of *Escherichia coli* in batch and continuous cultures. *J Gen Microbiol*, 135(11), 2875-2883. doi: 10.1099/00221287-135-11-2875
- Enfors, S. O., Jahic, M., Rozkov, A., Xu, B., Hecker, M., Jurgen, B., . . . Manelius, A. (2001). Physiological responses to mixing in large scale bioreactors. *J Biotechnol*, 85(2), 175-185.
- Eriksson, N. L. (2014). *Biochemical and Physiological Characterization of Nonsymbiotic Plant Hemoglobins*: Division of Pure and Applied Biochemistry, Lund University.
- Facultative anaerobic organism (2016, December 23). In Wikipedia, The Free Encyclopedia. Wikipedia, The Free Encyclopedia. Retrieved on 13 May 2017, from https://en.wikipedia.org/wiki/Facultative_anaerobic_organism
- Ferrer-Miralles, N., Domingo-Espin, J., Corchero, J. L., Vazquez, E., & Villaverde, A. (2009). Microbial factories for recombinant pharmaceuticals. *Microb Cell Fact*, 8, 17. doi: 10.1186/1475-2859-8-17
- Fronticelli, C., & Koehler, R. C. (2009). Design of recombinant hemoglobins for use in transfusion fluids. *Crit Care Clin*, 25(2), 357-371, Table of Contents. doi: 10.1016/j.ccc.2008.12.010
- Gallup, D. M., & Gerhardt, P. (1963). Dialysis Fermentor Systems for Concentrated Culture of Microorganisms. *Appl Microbiol*, 11(6), 506-512.
- Garrocho-Villegas, V., Gopalasubramaniam, S. K., & Arredondo-Peter, R. (2007). Plant hemoglobins: what we know six decades after their discovery. *Gene*, 398(1-2), 78-85. doi: 10.1016/j.gene.2007.01.035
- Han, K., Lim, H. C., & Hong, J. (1992). Acetic acid formation in *Escherichia coli* fermentation. *Biotechnol Bioeng*, 39(6), 663-671. doi: 10.1002/bit.260390611

- Hargrove, M. S., Brucker, E. A., Stec, B., Sarath, G., Arredondo-Peter, R., Klucas, R. V., . . . Phillips, G. N. (2000). Crystal structure of a nonsymbiotic plant hemoglobin. *Structure*, 8(9), 1005-1014.
- Hestrin, S., Avineri-Shapiro, S., & Aschner, M. (1943). The enzymic production of levan. *Biochem J*, 37(4), 450-456.
- Hill, R. D. (1998). What are hemoglobins doing in plants? *Canadian Journal of Botany*, 76(5), 707-712. doi: 10.1139/b98-057
- Hill, R. D. (2012). Non-symbiotic haemoglobins—What's happening beyond nitric oxide scavenging? *AoB Plants*, 2012. doi: 10.1093/aobpla/pls004
- Hochachka, P. W., Lutz, P. L., Sick, T. J., & Rosenthal, M. (1993). *Surviving hypoxia: Mechanisms of control and adaptation*: CRC Press.
- Hoy, J. A., & Hargrove, M. S. (2008). The structure and function of plant hemoglobins. *Plant Physiol Biochem*, 46(3), 371-379. doi: 10.1016/j.plaphy.2007.12.016
- Hoy, J. A., Robinson, H., Trent, J. T., 3rd, Kakar, S., Smagghe, B. J., & Hargrove, M. S. (2007). Plant hemoglobins: a molecular fossil record for the evolution of oxygen transport. *J Mol Biol*, 371(1), 168-179. doi: 10.1016/j.jmb.2007.05.029
- Hunt, P. W., Watts, R. A., Trevaskis, B., Llewelyn, D. J., Burnell, J., Dennis, E. S., & Peacock, W. J. (2001). Expression and evolution of functionally distinct haemoglobin genes in plants. *Plant Mol Biol*, 47(5), 677-692.
- Kakar, S., Hoffman, F. G., Storz, J. F., Fabian, M., & Hargrove, M. S. (2010). Structure and reactivity of hexacoordinate hemoglobins. *Biophys Chem*, 152(0), 1-14. doi: 10.1016/j.bpc.2010.08.008
- Kakar, S., Sturms, R., Tiffany, A., Nix, J. C., DiSpirito, A. A., & Hargrove, M. S. (2011). Crystal structures of Parasponia and Trema hemoglobins: differential heme coordination is linked to quaternary structure. *Biochemistry*, 50(20), 4273-4280. doi: 10.1021/bi2002423
- Kluger, R. (2010). Red cell substitutes from hemoglobin--do we start all over again? *Curr Opin Chem Biol*, 14(4), 538-543. doi: 10.1016/j.cbpa.2010.03.021
- Korz, D., Rinas, U., Hellmuth, K., Sanders, E., & Deckwer, W.-D. (1995). Simple fed-batch technique for high cell density cultivation of *Escherichia coli*. *Journal of biotechnology*, 39(1), 59-65.
- Kresie, L. (2001). Artificial blood: an update on current red cell and platelet substitutes. *Proc (Bayl Univ Med Cent)*, 14(2), 158-161.
- Lee, S. Y. (1996). High cell-density culture of *Escherichia coli*. *Trends Biotechnol*, 14(3), 98-105. doi: 10.1016/0167-7799(96)80930-9
- Leiva-Eriksson, N., Pin, P. A., Kraft, T., Dohm, J. C., Minoche, A. E., Himmelbauer, H., & Bulow, L. (2014). Differential expression patterns of non-symbiotic hemoglobins in

- sugar beet (*Beta vulgaris* ssp. *vulgaris*). *Plant Cell Physiol*, 55(4), 834-844. doi: 10.1093/pcp/pcu027
- Leiva-Eriksson, N., Reeder, B. J., Wilson, M. T. & Bülow, L. (2014a). Ligand binding in sugar beet nonsymbiotic hemoglobins. Division of Pure and Applied Biochemistry, Lund University.
- Majewski, R. A., & Domach, M. M. (1990). Simple constrained-optimization view of acetate overflow in *E. coli*. *Biotechnol Bioeng*, 35(7), 732-738. doi: 10.1002/bit.260350711
- Marisch, K., Bayer, K., Cserjan-Puschmann, M., Luchner, M., & Striedner, G. (2013). Evaluation of three industrial *Escherichia coli* strains in fed-batch cultivations during high-level SOD protein production. *Microb Cell Fact*, 12, 58. doi: 10.1186/1475-2859-12-58
- Marisch, K., Bayer, K., Cserjan-Puschmann, M., Luchner, M., & Striedner, G. (2013). Evaluation of three industrial *Escherichia coli* strains in fed-batch cultivations during high-level SOD protein production. *Microb Cell Fact*, 12(1), 58. doi: 10.1186/1475-2859-12-58
- Mot, A. C. (2014). Nonsymbiotic plant hemoglobins: Synopsis and perspectives of their structure and enzymatic activities. *Acta Metallomica - MEEMB, Tome XI*, Nos. 2-4, 163-169
- Murarka, A., Clomburg, J. M., Moran, S., Shanks, J. V., & Gonzalez, R. (2010). Metabolic analysis of wild-type *Escherichia coli* and a pyruvate dehydrogenase complex (PDHC)-deficient derivative reveals the role of PDHC in the fermentative metabolism of glucose. *J Biol Chem*, 285(41), 31548-31558. doi: 10.1074/jbc.M110.121095
- Ness, P. M., & Cushing, M. M. (2007). Oxygen therapeutics: pursuit of an alternative to the donor red blood cell. *Arch Pathol Lab Med*, 131(5), 734-741. doi: 10.1043/1543-2165(2007)131[734:otpoaa]2.0.co;2
- Perazzolli, M., Dominici, P., Romero-Puertas, M. C., Zago, E., Zeier, J., Sonoda, M., . . . Delledonne, M. (2004). Arabidopsis Nonsymbiotic Hemoglobin AHb1 Modulates Nitric Oxide Bioactivity. *Plant Cell*, 16(10), 2785-2794. doi: 10.1105/tpc.104.025379
- Plomer, J. J., Ryland, J. R., Matthews, M. A. H., Traylor, D. W., Milne, E. E., Durfee, S. L., . . . Neway, J. O. (1998). Purification of hemoglobin: Google Patents.
- Porphyrin. (2017, May 23). In *Wikipedia, The Free Encyclopedia*. Retrieved 15:21, July 12, 2017, from <https://en.wikipedia.org/w/index.php?title=Porphyrin&oldid=781762373>
- Reeder, B. J., & Hough, M. A. (2014). The structure of a class 3 nonsymbiotic plant haemoglobin from *Arabidopsis thaliana* reveals a novel N-terminal helical extension. *Acta Crystallogr D Biol Crystallogr*, 70(Pt 5), 1411-1418. doi: 10.1107/s1399004714004878
- Riesenberg, D. (1991). High-cell-density cultivation of *Escherichia coli*. *Curr Opin Biotechnol*, 2(3), 380-384.

- Riesenberg, D., & Guthke, R. (1999). High-cell-density cultivation of microorganisms. *Appl Microbiol Biotechnol*, 51(4), 422-430.
- Riesenberg, D., Menzel, K., Schulz, V., Schumann, K., Veith, G., Zuber, G., & Knorre, W. A. (1990). High cell density fermentation of recombinant *Escherichia coli* expressing human interferon alpha 1. *Appl Microbiol Biotechnol*, 34(1), 77-82.
- Ross, E. J. H., Lira-Ruan, V., Arredondo-Peter, R., Klucas, R. V. & Sarath, G. (2002). Recent insights into plant hemoglobin. Reviews in Plant Biochemistry and Biotechnology. Volume 1, pp.173 - 189.
- Sanders, K. E., Ackers, G., & Sligar, S. (1996). Engineering and design of blood substitutes. *Curr Opin Struct Biol*, 6(4), 534-540.
- Sarkar, S. (2008). Artificial blood. *Indian J Crit Care Med*, 12(3), 140-144. doi: 10.4103/0972-5229.43685
- Shiloach, J., & Bauer, S. (1975). High-yield growth of *E. coli* at different temperatures in a bench scale fermentor. *Biotechnol Bioeng*, 17(2), 227-239.
- Shiloach, J., & Fass, R. (2005). Growing *E. coli* to high cell density--a historical perspective on method development. *Biotechnol Adv*, 23(5), 345-357. doi: 10.1016/j.biotechadv.2005.04.004
- Smaghe, B. J., Hoy, J. A., Percifield, R., Kundu, S., Hargrove, M. S., Sarath, G., . . . Appleby, C. A. (2009). Review: correlations between oxygen affinity and sequence classifications of plant hemoglobins. *Biopolymers*, 91(12), 1083-1096. doi: 10.1002/bip.21256
- Smaghe, B. J., Sarath, G., Ross, E., Hilbert, J. L., & Hargrove, M. S. (2006). Slow ligand binding kinetics dominate ferrous hexacoordinate hemoglobin reactivities and reveal differences between plants and other species. *Biochemistry*, 45(2), 561-570. doi: 10.1021/bi0519021
- Soini, J., Ukkonen, K., & Neubauer, P. (2008). High cell density media for *Escherichia coli* are generally designed for aerobic cultivations - consequences for large-scale bioprocesses and shake flask cultures. *Microb Cell Fact*, 7, 26. doi: 10.1186/1475-2859-7-26
- Sorensen, H. P., & Mortensen, K. K. (2005). Advanced genetic strategies for recombinant protein expression in *Escherichia coli*. *J Biotechnol*, 115(2), 113-128. doi: 10.1016/j.jbiotec.2004.08.004
- Sowa, A. W., Duff, S. M. G., Guy, P. A., & Hill, R. D. (1998). Altering hemoglobin levels changes energy status in maize cells under hypoxia. *Proc Natl Acad Sci U S A*, 95(17), 10317-10321.
- Spyrakakis, F., Luque, F. J., & Viappiani, C. (2011). Structural analysis in nonsymbiotic hemoglobins: what can we learn from inner cavities? *Plant science*, 181(1), 8-13.
- Thiel, J., Rolletschek, H., Friedel, S., Lunn, J. E., Nguyen, T. H., Feil, R., . . . Borisjuk, L. (2011). Seed-specific elevation of non-symbiotic hemoglobin AtHb1: beneficial

- effects and underlying molecular networks in *Arabidopsis thaliana*. *BMC Plant Biol*, *11*, 48. doi: 10.1186/1471-2229-11-48
- Toyoda, K., Teramoto, H., Inui, M., & Yukawa, H. (2009). Molecular mechanism of SugR-mediated sugar-dependent expression of the *ldhA* gene encoding L-lactate dehydrogenase in *Corynebacterium glutamicum*. *Appl Microbiol Biotechnol*, *83*(2), 315-327. doi: 10.1007/s00253-009-1887-x
- Varnado, C. L., Mollan, T. L., Birukou, I., Smith, B. J., Henderson, D. P., & Olson, J. S. (2013). Development of recombinant hemoglobin-based oxygen carriers. *Antioxid Redox Signal*, *18*(17), 2314-2328. doi: 10.1089/ars.2012.4917
- Virtanen, A. I., & Laine, T. (1946). Red, brown and green pigment in leguminous root nodules. *Nature*, *157*, 25.
- Watts, R. A., Hunt, P. W., Hvitved, A. N., Hargrove, M. S., Peacock, W. J., & Dennis, E. S. (2001). A hemoglobin from plants homologous to truncated hemoglobins of microorganisms. *Proc Natl Acad Sci U S A*, *98*(18), 10119-10124. doi: 10.1073/pnas.191349198
- Winzer, K., Hardie, K. R., & Williams, P. (2002). Bacterial cell-to-cell communication: sorry, can't talk now - gone to lunch! *Curr Opin Microbiol*, *5*(2), 216-222.
- Xu, B., Jahic, M., Blomsten, G., & Enfors, S. O. (1999). Glucose overflow metabolism and mixed-acid fermentation in aerobic large-scale fed-batch processes with *Escherichia coli*. *Appl Microbiol Biotechnol*, *51*(5), 564-571.
- Yang, Y.-T., Bennett, G. N., & San, K.-Y. (1998). Genetic and metabolic engineering. *Electronic Journal of Biotechnology*, *1*, 20-21.
- Yee, L., & Blanch, H. W. (1992). Recombinant protein expression in high cell density fed-batch cultures of *Escherichia coli*. *Biotechnology (N Y)*, *10*(12), 1550-1556.
- Zabriskie, D. W., & Arcuri, E. J. (1986). Factors influencing productivity of fermentations employing recombinant microorganisms. *Enzyme and Microbial Technology*, *8*(12), 706-717. doi: [http://dx.doi.org/10.1016/0141-0229\(86\)90157-2](http://dx.doi.org/10.1016/0141-0229(86)90157-2)

APPENDICES

A1. The Inoue method for transformation of competent *Escherichia coli*

The following major changes were made from the protocol;

1. 2 μL (50 ng equivalent) of pBSK-*bv*hb1.1-cTP was transformed into 100 μL *E. coli* TG1 of competent cell.
2. 400 μL of LB medium was used instead of 800 μL of SOC. And the culture was not incubated for 45 minutes.

Protocol 24: The Inoue Method for Preparation and Transformation of Competent *E. coli* L.115

15. Use a chilled, sterile pipette tip to transfer the competent cells to chilled, sterile (7 x 105-mm polypropylene tubes. Store the cells on ice.
Glass tubes should not be used since they lower the efficiency of transformation by ~10-fold.

Transformation

Include all of the appropriate positive and negative controls (please see the panel on BACTERIAL TRANSFORMATION in Protocol 23).

16. Add the transforming DNA (up to 25 ng per 50 μL of competent cells) in a volume not exceeding 5% of that of the competent cells. Swirl the tubes gently several times to mix their contents. Set up at least two control tubes for each transformation experiment, including a tube of competent bacteria that receives a known amount of a standard preparation of superhelical plasmid DNA and a tube of cells that receives no plasmid DNA at all. Store the tubes on ice for 30 minutes.
17. Transfer the tubes to a rack placed in a preheated 42°C circulating water bath. Store the tubes in the rack for exactly 90 seconds. Do not shake the tubes.
Heat shock is a crucial step. It is very important that the cells be raised to exactly the right temperature at the correct rate. The incubation times and temperatures given here have been worked out using Falcon 2089 tubes. Other types of tubes will not necessarily yield equivalent results.
18. Rapidly transfer the tubes to an ice bath. Allow the cells to cool for 1-2 minutes.
19. Add 800 μL of SOC medium to each tube. Warm the cultures to 37°C in a water bath, and then transfer the tubes to a shaking incubator set at 37°C. Incubate the cultures for 45 minutes to allow the bacteria to recover and to express the antibiotic resistance marker encoded by the plasmid.
To maximize the efficiency of transformation, gently agitate (<225 cycles/minute) the cells during the recovery period.
If necessary, to complementation, proceed to Protocol 27 for plating.
20. Transfer the appropriate volume (up to 200 μL per 90-mm plate) of transformed competent cells onto agar SOB medium containing 20 mM MgSO_4 and the appropriate antibiotic.
When selecting for resistance to tetracycline, the entire transformation mixture may be spread on a single plate (or plated in triplicate). In this case, collect the biomass by centrifuging for 20 seconds at room temperature in a microtube, and then gently resuspend the cell pellet in 100 μL of SOC medium by tapping the sides of the tube.
▲ IMPORTANT: Swirl a heat glass rod by dipping it into ethanol and then in the flame of a Bunsen burner. When the rod has cooled to room temperature, spread the transformed cells gently over the surface of the agar plate.
When selecting for resistance to ampicillin, transformed cells should be plated at low density (<10⁶ colonies per 90-mm plate), and the plate should not be incubated for more than 20 hours at 30°C. The enzyme β -lactamase is secreted into the medium from ampicillin resistant transformants and can rapidly inactivate the antibiotic molecules surrounding the colonies. Thus, plating cells at high density or incubating them for long periods of time results in the appearance of ampicillin-sensitive colonies. This problem is ameliorated, but not completely eliminated, by using carbenicillin (not ampicillin) in selective media and increasing the concentration of antibiotic from 60 $\mu\text{g/ml}$ to 100 $\mu\text{g/ml}$. The number of ampicillin-resistant colonies does not increase in linear proportion to the number of cells applied to the plate, perhaps because of growth-inhibiting substances released from the cells killed by the antibiotic.
21. Store the plates at room temperature until the liquid has been absorbed.
22. Invert the plates and incubate them at 37°C. Transformed colonies should appear in 12-16 hours.

Transformed colonies may be screened for the presence of recombinant plasmids using one of the methods described in Protocols 27, 28, 31, and 32 of this chapter or Protocol 12 in Chapter 4.

A2. Isolation of high-copy plasmid DNA from *E. coli*

NucleoSpin Plasmid isolation and purification kit

1. 5 ml of overnight *E. coli* culture was centrifuged at 12,000 rpm for 1 min. The supernatant was discarded and pellet kept.
2. The pellet was resuspended completely in 250 µl of buffer A1 by pipetting up and down.
3. Thereafter, 250 µl of buffer A2 was added and the mixture was mixed by inverting the tube for 6 times. Then, the mixture was incubated at room temperature for 12 minutes to obtain a clear lysate. Buffer A3 (300 µl) was added and the mixture mixed by inverting 8 times to get a colourless mixture, and centrifuged for 5 min at 12,000 rpm.
4. The clear supernatant was carefully transferred into a NucleoSpin Plasmid column and centrifuged for 1 minute at 12,000 rpm. Flow-through was discarded.
5. Plasmid DNA was first washed with 500 µl of buffer AW by centrifuging at 12,000 rpm for 1 minute. And then 600 µl of Buffer A4 supplemented with ethanol was added and centrifuged for 1 minute at 12,000 rpm. The flow-through was discarded.
6. The tube was centrifuged again for 2 min at 12,000 rpm and the flow-through discarded.
7. Lastly, the NucleoSpin Plasmid tube was placed in a 1.5 mL microcentrifuge tube and 50 µl of buffer AE added two subsequent times and centrifuged for 1 minutes at 12,000 rpm to elute the plasmid DNA. The flow-through was used to determine the concentration of plasmid DNA obtained.

Sample was later stored at -20 °C until use

Isolation of high-copy plasmid DNA from *E. coli*

Before starting the preparation:

- Check if Wash Buffer A4 was prepared according to section 3.

1 Cultivate and harvest bacterial cells

Use **1–5 mL** of a saturated *E.coli* **LB culture**, pellet cells in a standard benchtop microcentrifuge for **30 s** at **11,000 x g**. Discard the supernatant and remove as much of the liquid as possible.



**11,000 x g,
30 s**

Note: For isolation of low-copy plasmids refer to section 5.2.

2 Cell lysis

Add **250 µL Buffer A1**. Resuspend the cell pellet completely by vortexing or pipetting up and down. Make sure no cell clumps remain before addition of Buffer A2!

**+ 250 µL A1
Resuspend**

Attention: Check Buffer A2 for precipitated SDS prior to use. If a white precipitate is visible, warm the buffer for several minutes at 30–40 °C until precipitate is dissolved completely. Mix thoroughly and cool buffer down to room temperature (18–25 °C).



**+ 250 µL A2
Mix**

Add **250 µL Buffer A2**. Mix gently by inverting the tube **6–8 times**. Do not vortex to avoid shearing of genomic DNA. Incubate at **room temperature** for up to **5 min** or until lysate appears clear.

RT, 5 min

Add **300 µL Buffer A3**. Mix thoroughly by inverting the tube **6–8 times** until blue samples turn colorless completely! Do not vortex to avoid shearing of genomic DNA!

**+ 300 µL A3
Mix**

Make sure to neutralize completely to precipitate all protein and chromosomal DNA. LyseControl should turn completely colorless without any traces of blue.

3 Clarification of lysate

Centrifuge for **5 min** at **11,000 x g** at room temperature.

Repeat this step in case the supernatant is not clear!



**11,000 x g,
5–10 min**

4 Bind DNA

Place a NucleoSpin® Plasmid / Plasmid (NoLid) Column in a Collection Tube (2 mL) and decant the supernatant from step 3 or pipette a maximum of 750 µL of the supernatant onto the column. Centrifuge for **1 min** at **11,000 x g**. Discard flow-through and place the NucleoSpin® Plasmid / Plasmid (NoLid) Column back into the collection tube.

**Load
supernatant****11,000 x g,
1 min**

Repeat this step to load the remaining lysate.

5 Wash silica membrane

*Recommended: If plasmid DNA is prepared from host strains containing high levels of nucleases (e.g., HB101 or strains of the JM series), it is **strongly recommended** performing an additional washing step with **500 µL Buffer AW**, optionally preheated to **50 °C**, and centrifuge for **1 min** at **11,000 x g** before proceeding with Buffer A4. Additional washing with Buffer AW will also increase the reading length of DNA sequencing reactions and improve the performance of critical enzymatic reactions.*

**Optional:
+ 500 µL AW****11,000 x g,
1 min**

Add **600 µL Buffer A4** (supplemented with ethanol, see section 3). Centrifuge for **1 min** at **11,000 x g**. Discard flow-through and place the NucleoSpin® Plasmid / Plasmid (NoLid) Column back into the **empty** collection tube.

**+ 600 µL A4
11,000 x g,
1 min**

6 Dry silica membrane

Centrifuge for **2 min** at **11,000 x g** and discard the collection tube.



Note: Residual ethanolic wash buffer might inhibit enzymatic reactions.

**11,000 x g,
2 min**

7 Elute DNA

Place the NucleoSpin® Plasmid / Plasmid (NoLid) Column in a 1.5 mL microcentrifuge tube (not provided) and add **50 µL Buffer AE**. Incubate for **1 min** at **room temperature**. Centrifuge for 1 min at **11,000 x g**.

Note: For more efficient elution procedures and alternative elution buffer (e.g., TE buffer or water) see section 2.5.

A3. Gateway Technology BP Recombination Reaction

BP recombination reaction mix

Components	Sample tube (μl)	Negative control (μl)	Positive control (μl)
attB-bvhb1.1-cTP (24.85 ng/μl)	3.5	3.5	-
pDONR vector (150 ng/μl)	1	-	1
TE buffer, pH 8.0	3.5	6.5	5
BP Clonase II enzyme mix	2	-	2
pEXT7-tet	-	-	2

Performing the BP Recombination Reaction

Setting Up the BP Recombination Reaction

1. Add the following components to 1.5 ml microcentrifuge tubes at room temperature and mix.

Note: To include a negative control, set up a second sample reaction and omit the BP Clonase™ II enzyme mix (see Step 4).

Components	Sample	Positive Control	Negative Control
<i>attB</i> -PCR product or linearized <i>attB</i> expression clone (20-50 fmol)	1-7 μl	--	1-7 μl
pDONR™ vector (150 ng/μl)	1 μl	1 μl	1 μl
pEXP7-tet positive control (50 ng/μl)	--	2 μl	--
TE Buffer, pH 8.0	to 8 μl	5 μl	to 10 μl

2. Remove the BP Clonase™ II enzyme mix from -20°C and thaw on ice (~ 2 minutes).
3. Vortex the BP Clonase™ II enzyme mix briefly twice (2 seconds each time).
4. Add 2 μl of BP Clonase™ II enzyme mix to the sample and positive control vials. Do not add BP Clonase™ II to the negative control vial. Mix well by vortexing briefly twice (2 seconds each time).

Reminder: Return BP Clonase™ II enzyme mix to -20°C immediately after use.

5. Incubate reactions at 25°C for 1 hour.

Note: For most applications, a 1 hour incubation will yield a sufficient number of entry clones. Depending on your needs, the length of the recombination reaction can be extended up to 18 hours. An overnight incubation typically yields 5-10 times more colonies than a 1 hour incubation. For large PCR products (≥5 kb), longer incubations (*i.e.* overnight incubation) will increase the yield of colonies and are recommended.

6. Add 1 μl of the Proteinase K solution to each reaction. Incubate for 10 minutes at

37°C.

7. Proceed to **Transforming Competent Cells**, next page.

Note: You may store the BP reaction at -20°C for up to 1 week before transformation, if desired.

A4. Gateway Technology LR Recombination Reaction

LR recombination reaction mix

Components	Sample tube (μl)	Negative control (μl)	Positive control (μl)
Entry clone	5	5	-
Destination vector	1	1	1
TE buffer, pH 8.0	2	4	5
LR Clonase II enzyme mix	2	-	2
pENTR-gus	-	-	2

Setting Up the LR Recombination Reaction

1. Add the following components to 1.5 ml microcentrifuge tubes at room temperature and mix.

Note: To include a negative control, set up a second sample reaction and omit the LR Clonase™ II enzyme mix (see Step 4).

Component	Sample	Negative Control	Positive Control
Entry clone (50-150 ng/reaction)	1-7 μ l	1-7 μ l	--
Destination vector (150 ng/ μ l)	1 μ l	1 μ l	1 μ l
pENTR™-gus (50 ng/ μ l)	--	--	2 μ l
TE Buffer, pH 8.0	to 8 μ l	to 10 μ l	5 μ l

2. Remove the LR Clonase™ II enzyme mix from -20°C and thaw on ice (~ 2 minutes).
3. Vortex the LR Clonase™ II enzyme mix briefly twice (2 seconds each time).
4. Add 2 μ l of LR Clonase™ II enzyme mix to the sample and positive control vials. Do not add LR Clonase™ II enzyme mix to the negative control vial. Mix well by vortexing briefly twice (2 seconds each time).

Reminder: Return LR Clonase™ II enzyme mix to -20°C immediately after use.

5. Incubate reactions at 25°C for 1 hour.

Note: For most applications, 1 hour will yield a sufficient number of colonies for analysis. Depending on your needs, the length of the recombination reaction can be extended up to 18 hours. For large plasmids (≥ 10 kb), longer incubation times (*i.e.* overnight incubation) will yield more colonies and are recommended.
6. Add 1 μ l of the Proteinase K solution to each reaction. Incubate for 10 minutes at 37°C.
7. Proceed to transform a suitable *E. coli* host and select for expression clones. To transform One Shot® OmniMAX™ 2-T1^R *E. coli*, follow the protocol on page 24.

Note: You may store the LR reaction at -20°C for up to 1 week before transformation, if desired.

A5. DNA Extraction from Agarose gel

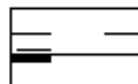
5.2 DNA extraction from agarose gels

Before starting the preparation:

- Check if Wash Buffer NT3 was prepared according to section 3.

1 Excise DNA fragment / solubilize gel slice

Note: Minimize UV exposure time to avoid damaging the DNA. Refer to section 2.5 for more tips on agarose gel extraction.



Take a clean scalpel to excise the DNA fragment from an agarose gel. Remove all excess agarose.

! Determine the weight of the gel slice and transfer it to a clean tube.

For each 100 mg of agarose gel < 2% add 200 μ L Buffer NT1.



+ 200 μ L NT1
per
100 mg gel

For gels containing > 2% agarose, double the volume of Buffer NT1.

Incubate sample for 5–10 min at 50 °C. Vortex the sample briefly every 2–3 min until the gel slice is completely dissolved!

50 °C
5–10 min

2 Bind DNA

Place a NucleoSpin[®] Gel and PCR Clean-up Column into a Collection Tube (2 mL) and load up to 700 μ L sample.



Load sample

Centrifuge for 30 s at 11,000 x g. Discard flow-through and place the column back into the collection tube.

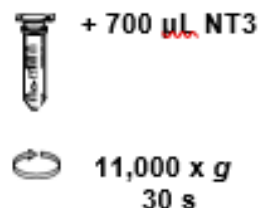


11,000 x g
30 s

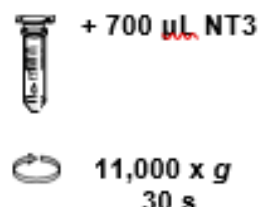
Load remaining sample if necessary and repeat the centrifugation step.

3 Wash silica membrane

Add 700 μL Buffer NT3 to the NucleoSpin[®] Gel and PCR Clean-up Column. Centrifuge for 30 s at 11,000 x g. Discard flow-through and place the column back into the collection tube.



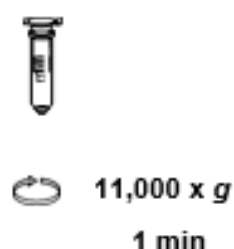
Recommended: Repeat previous washing step to minimize chaotropic salt carry-over and low A_{260}/A_{230} (see section 2.7 for detailed information).



4 Dry silica membrane

Centrifuge for 1 min at 11,000 x g to remove Buffer NT3 completely. Make sure the spin column does not come in contact with the flow-through while removing it from the centrifuge and the collection tube.

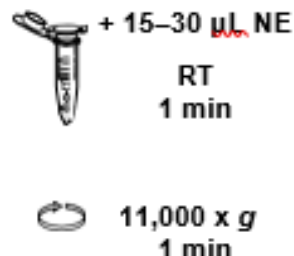
Note: Residual ethanol from Buffer NT3 might inhibit enzymatic reactions. Total removal of ethanol can be achieved by incubating the columns for 2–5 min at 70 °C prior to elution.



5 Elute DNA

Place the NucleoSpin[®] Gel and PCR Clean-up Column into a new 1.5 mL microcentrifuge tube (not provided). Add 15–30 μL Buffer NE and incubate at room temperature (18–25 °C) for 1 min. Centrifuge for 1 min at 11,000 x g.

Note: DNA recovery of larger fragments (> 1000 bp) can be increased by multiple elution steps with fresh buffer, heating to 70 °C and incubation for 5 min. See section 2.6 for detailed information.



A6. One Shot Chemical Transformation Protocol

One Shot[®] Chemical Transformation Protocol

Use this procedure to transform the BP recombination reaction into One Shot[®] OmniMAX™ 2-T1^R chemically competent *E. coli*. If you are using another *E. coli* strain, follow the manufacturer's instructions.

1. Thaw, on ice, one vial of One Shot[®] OmniMAX™ 2-T1^R chemically competent cells for each transformation.
2. Add 1 µl of the BP recombination reaction (from **Performing the BP Recombination Reaction**, Step 7, page 22) into a vial of One Shot[®] OmniMAX™ 2-T1^R cells and mix gently. **Do not mix by pipetting up and down.** For the pUC19 control, add 10 pg (1 µl) of DNA into a separate vial of One Shot[®] cells and mix gently.
3. Incubate the vial(s) on ice for 30 minutes.
4. Heat-shock the cells for 30 seconds at 42°C without shaking.
5. Remove the vial(s) from the 42°C bath and place them on ice for 2 minutes.
6. Add 250 µl of room temperature S.O.C. medium to each vial.
7. Cap the vial(s) tightly and shake horizontally (225 rpm) at 37°C for 1 hour.
8. Before plating, dilute the transformation mix 1:10 into LB Medium (e.g. remove 20 µl of the transformation mix and add to 180 µl of LB Medium)
9. Spread 20 µl and 100 µl from each transformation on a prewarmed selective plate and incubate overnight at 37°C. We recommend plating 2 different volumes to ensure that at least 1 plate has well-spaced colonies.

An efficient BP recombination reaction may produce hundreds of colonies (> 1500 colonies if the entire BP reaction is transformed and plated).

A7. Fermenter on-line pH and dissolved oxygen calibration procedure

Calibration of the pH probe

1. Connect the probe with the cable connected to the fermenter unit. The calibration is performed before inserting the probe into the fermenter vessel.
2. Start the software and click on master panel
3. Rinse the probe with distilled water. Do not dry.
4. Insert the probe into the pH 7.00 buffer solution
5. Press Calibrate -> pH -> tcomp -> manuell -> temp -> ok -> mode meas -> calibration
6. Type pH 7.00 and press Ok. Leave the sensor inside for 60 sec. Afterwards press Stop calib. (check the ELEC, standard for pH 7.00 is 6 nA)
7. Remove the sensor, rinse it with water and repeat the previous step with the pH 4.01 buffer. (check the ELEC, standard for pH 4.01 is 181 nA).
8. In case of an Error signal, repeat the calibration procedure one more time.

Calibration of DO probe

1. Connect the probe with the cable connected to the fermenter unit. The probe has to be polarized before calibration. The polarization takes at least **6h**. The calibration is performed before inserting the probe into the fermenter vessel.
2. Rinse the probe with distilled water and dry carefully. Make sure not to touch the sensor with bare hands. Place the probe secure to the holder in the open air. Avoid exposing the sensor to strong air currents.
3. Press Calibrate → DO → tcomp → manuell → temp → ok → mode meas → calibration → Calib with air
4. Check the ELEC value (nA) and calculate the correct percentage of air that corresponds to that value. This will be based on estimation that 69 nA is equivalent to 100 %.
5. Press OK on the computer and leave the probe calibrating for exactly 60 sec. Finish by pressing Stop calib.

Recalibration procedure:

1. On the program control, click Calibration → pH → mode meas → recalib. Then type the actual pH and OK.
2. For DO sensor recalibration, increase the pO₂ set point to 100 % and the aeration level to 11 litre/min. Then, allow the medium to stirrer for about 5 min. or until the DO sensor stabilizes.

A8. Multiplication factors for addition of a 100 % Saturated Solution of Ammonium Sulfate.

Multiplication Factors for Addition of a 100% Saturated Solution of Ammonium Sulfate.

The table below provides multiplication factors for use in calculating the required volume of a 100% saturated ammonium sulfate solution. The table values are independent of temperature.

		Desired Final Ammonium Sulfate Percent Saturation																	
		10	15	20	25	30	35	40	45	50	55	60	65	70	75	80	85	90	95
Initial Ammonium Sulfate Percent Saturation	0	0.111	0.176	0.250	0.333	0.429	0.538	0.667	0.818	1.000	1.222	1.500	1.857	2.333	3.000	4.000	5.667	9.000	19.000
	10		0.059	0.125	0.200	0.286	0.385	0.500	0.636	0.800	1.000	1.250	1.571	2.000	2.600	3.500	5.000	8.000	17.000
	15			0.063	0.133	0.214	0.308	0.417	0.545	0.700	0.889	1.125	1.429	1.833	2.400	3.250	4.667	7.500	16.000
	20				0.067	0.143	0.231	0.333	0.455	0.600	0.778	1.000	1.286	1.667	2.200	3.000	4.333	7.000	15.000
	25					0.071	0.154	0.250	0.364	0.500	0.667	0.875	1.143	1.500	2.000	2.750	4.000	6.500	14.000
	30						0.077	0.167	0.273	0.400	0.556	0.750	1.000	1.333	1.800	2.500	3.667	6.000	13.000
	35							0.083	0.182	0.300	0.444	0.625	0.857	1.167	1.600	2.250	3.333	5.500	12.000
	40								0.091	0.200	0.333	0.500	0.714	1.000	1.400	2.000	3.000	5.000	11.000
	45									0.100	0.222	0.375	0.571	0.833	1.200	1.750	2.667	4.500	10.000
	50										0.111	0.250	0.429	0.667	1.000	1.500	2.333	4.000	9.000
	55											0.125	0.286	0.500	0.800	1.250	2.000	3.500	8.000
	60												0.143	0.333	0.600	1.000	1.667	3.000	7.000
	65													0.167	0.400	0.750	1.333	2.500	6.000
	70														0.200	0.500	1.000	2.000	5.000
	75															0.250	0.667	1.500	4.000
	80																0.333	1.000	3.000
	85																	0.500	2.000
	90																		1.000
	95																		

A9. Molar extinction coefficients of sugar beet hemoglobin proteins

	BvHb1.1		BvHb1.2		BvHb2	
	λ_{\max}	$\epsilon(\text{mM}^{-1}\cdot\text{cm}^{-1})$	λ_{\max}	$\epsilon(\text{mM}^{-1}\cdot\text{cm}^{-1})$	λ_{\max}	$\epsilon(\text{mM}^{-1}\cdot\text{cm}^{-1})$
Ferrous Hb	423	137.9	424	112.5	424	168.3
	528	13.4	528; 533	9.2; 9.1	527	14.4
	555	19.8	555; 560	12.4; 12.8	557	25.6
Carboxy-Hb	416	144.7	416	101.4	415	183.1
	536	12.4	537	8.3	537	13.6
	566	12	566	7.8	564	13.6
Oxy-Hb	411	115.2	410	47.8	409	90.9
	538	13.5	539	6.4	538	10.5
	574	11.2	574	4.9	574	6.9
Ferric Hb	409	121.5	407	91.9	408	128
	532	12.2	530	7.4	533	11.7

A10. Pyridine hemochromagen method

SPECTROPHOTOMETRIC HEME ASSAY OF PYRIDINE HEMOCHROME

In this assay the nitrogen ligands from protein-bound heme are replaced by pyridine in alkali. The resultant hemochrome is quantitated by the difference spectrum of the reduced and oxidized compound. The sensitivity of the assay is a function of the sensitivity of the spectrophotometer and of the ability to use microcells for minimal volumes.

CAUTION: Due to the toxicity and odor of pyridine, the procedure should be performed in a hood as much as possible and cuvettes should be capped or sealed with Parafilm.

Materials

5% (w/v) tissue sample suspension: tissue homogenate, or a homogenate or sonicate of tissue culture cells (minimally, 2 mg protein)

Reagent-grade pyridine (discard if yellow)

1.0 M NaOH

Sodium dithionite crystals

3 M potassium ferricyanide

12 × 75-mm disposable glass tubes (Fisher)

Sensitive scanning spectrophotometer

Appropriate cuvettes with caps

1. Place 0.84 ml of 5% (w/v) aqueous tissue sample suspension in a 12 × 75-mm disposable glass tube.

The volumes given throughout the assay can be reduced or increased proportionately.

2. Add 0.2 ml reagent-grade pyridine and mix by vortexing.
3. Add 0.1 ml of 1 M NaOH and mix thoroughly by vortexing.

In tissue culture assays, NaOH can be replaced by 0.16 M sodium borate, pH 9.0.

4. Split the sample between two cuvettes and obtain a baseline absorbance spectrum from 500 to 600 nm.
5. Using the tip of a fine spatula, add a few crystals of sodium dithionite and 0.01 ml water to one cuvette and mix to reduce hemochrome.

BASIC PROTOCOL

Heme Synthesis
Pathway

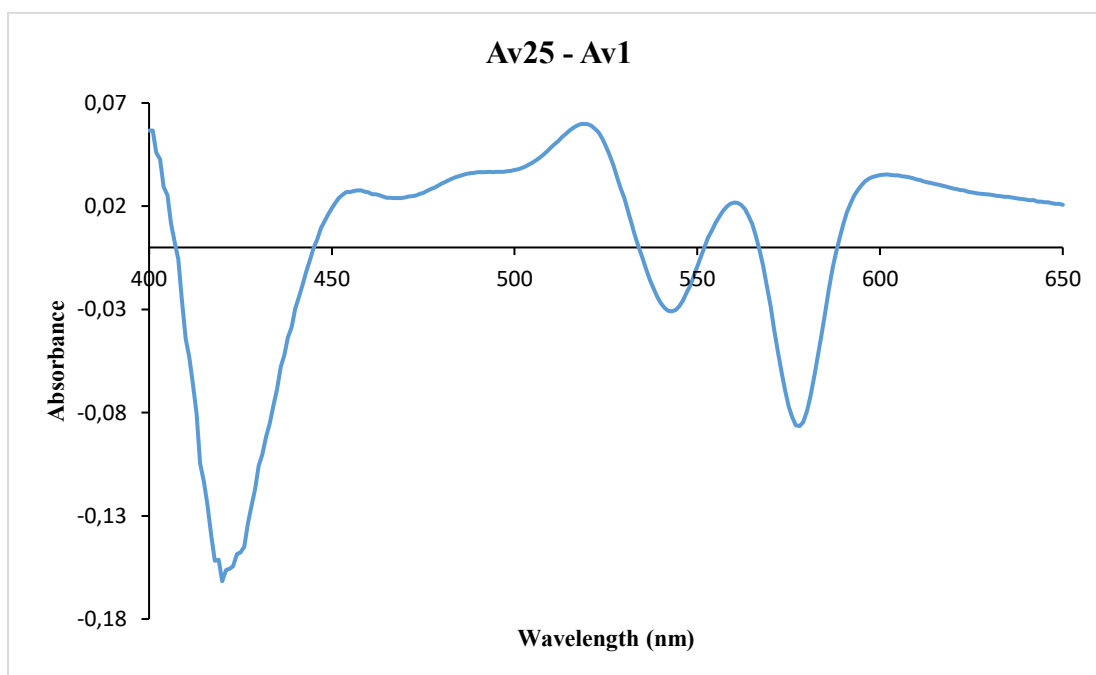
A11. Glucose feeding profiles used for BvHbs fermentation.

In-house determined (for human Hb)		BvHb1.1-cTP_170118		BvHb1.1-cTP_170126		BvHb1.1-cTP_170215	
Time Interval (hr)	Glucose profile (%)	Time interval (hr)	Glucose profile (%)	Time interval (hr)	Glucose profile (%)	Time interval (hr)	Glucose profile (%)
01:00	1.0	01:00	1.0	01:00	1.0	01:00	1.0
03:00	3.0	03:00	3.0	03:00	3.0	03:00	3.0
07:00	1.0	07:00	4.0	07:00	4.0	07:00	4.0
10:00	2.0	10:00	3.0	10:00	3.0	10:00	3.0
14:00	1.0	14:00	1.5	14:00	1.5	14:00	1.5
18:00	2.0	18:00	2.0	18:00	1.0	18:00	2.0
22:00	1.0	22:00	1.5	22:00	2.0	22:00	1.0
25:00	2.0	24:00	1.5	24:00	0.8	24:00	2.0
27:00	1.0	28:00	2.0	28:00	0.8	28:00	1.0
30:00	2.0	30:00	1.5	30:00	1.0	30:00	2.0

In-house determined (for human Hb)		BvHb1.2_160906		BvHb1.2_161109		BvHb1.2_170220	
Time Interval (hr)	Glucose profile (%)	Time interval (hr)	Glucose profile (%)	Time interval (hr)	Glucose profile (%)	Time interval (hr)	Glucose profile (%)
01:00	1.0	01:00	1.0	01:00	1.0	07:00	1.0
03:00	3.0	03:00	3.0	03:00	3.0	09:00	3.0
07:00	1.0	07:00	1.0	07:00	4.0	14:00	1.0
10:00	2.0	10:00	2.0	10:00	2.0	17:00	2.0
14:00	1.0	14:00	1.0	14:00	1.5	21:00	1.0
18:00	2.0	18:00	2.0	18:00	2.0	25:00	2.0
22:00	1.0	22:00	1.0	22:00	2.0	29:00	1.0
25:00	2.0	25:00	2.0	24:00	1.5	33:00	2.0
27:00	1.0	27:00	1.0	28:00	2.0	37:00	1.0
30:00	2.0	30:00	2.0	30:00	1.5	41:00	2.0

In-house determined (for human Hb)		BvHb2_161025		BvHb2_161104		BvHb2_170227	
Time Interval (hr)	Glucose profile (%)	Time interval (hr)	Glucose profile (%)	Time interval (hr)	Glucose profile (%)	Time interval (hr)	Glucose profile (%)
01:00	1.0	01:00	1.0	01:00	1.0	05:00	0.0
03:00	3.0	03:00	3.0	03:00	3.0	07:00	2.0
07:00	1.0	07:00	1.0	07:00	4.0	09:00	3.0
10:00	2.0	10:00	2.0	10:00	2.0	14:00	1.0
14:00	1.0	14:00	1.0	14:00	1.0	18:00	2.0
18:00	2.0	18:00	2.0	18:00	2.0	22:00	1.0
22:00	1.0	22:00	1.0	22:00	1.0	27:00	2.0
25:00	2.0	25:00	2.0	254:00	2.0	31:00	1.0
27:00	1.0	27:00	1.0	28:00	1.0	36:00	2.0
30:00	2.0	30:00	2.0	30:00	2.0	40:00	1.0

A12. BvHb1.2 autoxidation absorption spectra changes across 400 – 650 nm at 37 °C.



A13. BvHb1.2 autoxidation absorption spectra changes across 400 – 650 nm at 20 °C.

